

1 **Rare earth element resources on Fuerteventura, Canary**
2 **Islands, Spain: a geochemical and mineralogical approach**

3

4 Marc Campeny¹, Inmaculada Menéndez², Luis Quevedo^{2,3}, Jorge Yepes², Ramón
5 Casillas⁴, Agustina Ahijado⁴, Jorge Méndez-Ramos³, José Mangas²

6

7 ¹ Departament de Mineralogia, Museu de Ciències Naturals de Barcelona, Passeig Picasso s/n, 08003
8 Barcelona, Spain

9 ² Instituto de Oceanografía y Cambio Global, IOCG, Universidad de Las Palmas de Gran Canaria, 35017
10 Las Palmas de Gran Canaria, Spain

11 ³ Instituto de Materiales y Nanotecnología, Departamento de Física, Universidad de La Laguna, apartado
12 correos 456, 38200 La Laguna, Tenerife, Spain

13 ⁴ Departamento de Biología Animal, Edafología y Geología, Universidad de La Laguna, apartado correos
14 456, 38200 La Laguna, Tenerife, Spain.

15

16

17 *Correspondence to:* Marc Campeny (mcampenyc@bcn.cat)

18 **Abstract.** Rare earth elements (REEs) play a pivotal role in the ongoing energy and mobility transition
19 challenges. Given their critical importance, governments worldwide and especially from the European
20 Union, are actively promoting the exploration of REE resources. In this context, alkaline magmatic rocks
21 (including trachytes, phonolites, syenites, melteigites and ijolites), carbonatites and their associated
22 weathering products were subjected to a preliminary evaluation as potential targets for REE exploration on
23 Fuerteventura Island (Canary Archipelago, Spain) based on mineralogical and geochemical studies. These
24 lithologies show significant REE concentrations. However, only carbonatites exhibit the potential to host
25 economically viable REE mineral deposits. REE concentrations in carbonatites of about 10,300 ppm REY
26 (REEs plus yttrium) have been detected, comparable to other locations hosting significant deposits of these
27 critical elements worldwide. Conversely, alkaline magmatic rocks and the resulting weathering products
28 display limited REE contents. Notably, REEs in carbonatites are associated with primary accessory phases
29 such as REE-bearing pyrochlore and britholite, and secondary monazite. The carbonatites of Fuerteventura
30 hold promise as prospective REE deposits within a non-conventional geological setting (oceanic island).
31 However, due to intricate structural attributes, the irregular distribution of these mineralizations and
32 possible land use and environmental constraints, additional future detailed investigations are imperative to
33 ascertain their viability as substantial REE resources.

34
35
36 **Keywords.** Rare earth elements, Carbonatites, Fuerteventura, Canary Islands, Weathering

37 **1 Introduction**

38 The implementation of actions to mitigate climate change is one of the major global challenges facing
39 society today. In this regard, the European Commission (EC) has adopted a series of economic and
40 technological proposals aimed at reducing greenhouse gas emissions and transforming Europe into the first
41 climate-neutral continent by 2050. These guiding principles, encompassed in the European Green Deal
42 (EGD) (European Commission, 2019), are directly linked to the establishment of an energy and mobility
43 transition based on green technologies that will replace the current fossil fuel-based model. However, in
44 order to achieve the ambitious targets, other finite resources will be essential: metals. Some of them,
45 commonly referred to as *green metals*, will play a crucial role in a successful energy and mobility transition
46 and, consequently, in achieving the neutrality goals outlined by the EGD (Graedel et al., 2015; Jyothi et al.,
47 2020). Among the green metals is the group of rare earth elements (REEs) that are critical for a wide range
48 of high-tech applications such as wind turbines, electric vehicles, rechargeable batteries, energy-efficient
49 lighting, optical telecommunications, photovoltaic cells, solar energy harvesting or artificial photosynthesis
50 for “green hydrogen” (H₂) generation (Méndez-Ramos et al., 2013; Acosta-Mora et al., 2018; Wondraczek
51 et al., 2015). Such elements are also commonly known as the *vitamins of modern industry* (Alonso et al.,
52 2012; Chakhmouradian and Wall, 2012; Massari and Ruberti, 2013; Charalampides et al., 2015; Weng et
53 al., 2015; Balaram, 2019).

54 According to the International Union of Pure and Applied Chemistry (IUPAC), REEs comprise a group of
55 17 chemical elements: scandium (Sc), yttrium (Y) and the 15 members of the lanthanide series (Connelly
56 et al., 2005). The term “rare” is confusing because, even though REEs seldom occur in pure mineral phases,
57 their average concentration in the Earth’s crust is around 125 ppm, surpassing other common industrial
58 metals such as copper, gold or platinum (Long et al., 2010; Rudnick and Gao, 2014).

59 Given their pivotal role in modern industry and green technologies, as well as the projected increase in
60 demand for REEs in the coming years, governments worldwide are actively promoting the exploration of
61 new REE resources (Barteková and Kemp, 2016). In line with this, the EC included light rare earth elements
62 (LREEs) and heavy rare earth elements (HREEs) in the 2023 list of critical raw materials (CRMs),
63 acknowledging them as essential and considering HREEs as the material with the highest supply risk
64 (European Commission, 2023a).

65 On March 16, 2023, the EC presented a bold initiative to the European Parliament: The European Critical
66 Raw Materials Act. This regulation aims to establish a comprehensive framework to ensure a secure and
67 sustainable supply of CRMs, including REEs, in the coming years (European Commission, 2023b).

68 The search for REEs in the geological environment has primarily centred on investigating non-conventional
69 HREE sources such as soils and weathering products (Braun et al., 1993; Wang et al., 2010, Wang et al.,
70 2013; Berger et al., 2014; Aiglsperger et al., 2016; Torró et al., 2017; Reinhardt et al., 2018; Borst et al.,
71 2020), but also traditional and well-known LREE-bearing lithologies, such as carbonatites (Goodenough et
72 al., 2016; Yang et al., 2019; Pirajno and Yu, 2022).

73 Carbonatites are igneous rocks formed by carbonate mantle melts and are genetically associated with a
74 wide range of mafic, ultramafic, and alkaline silicate rocks (Yaxley et al., 2002). Although carbonates such
75 as calcite or dolomite are their main forming minerals, a significant portion of carbonatites contain
76 accessory phases enriched in critical metals such as REEs (Christy et al., 2021). REEs can be contained in
77 fluorcarbonates (e.g., bastnäsite, parisite, huanghoite, synchysite), phosphates (e.g., monazite,
78 rhabdophane), silicates (e.g., allanite), or even oxides (e.g., REE-bearing pyrochlore, cerianite). These
79 accessory minerals make carbonatites the main current REE source, representing 86.5% of the deposits
80 under exploitation for these elements (Liu et al., 2023). However, although carbonatites are rare rocks,
81 predominantly found in continental rifts associated with cratons (Humphreys-Williams et al., 2021), they
82 have exceptionally been described in other geological contexts, most notably oceanic islands associated
83 with hotspots, such as Cape Verde (Mourão et al., 2010; De Ignacio et al., 2018;) or Fuerteventura in the
84 Canary Islands (Mangas et al., 1996; Carnevale et al., 2021).

85 The petrogenesis of carbonatites is still a debated topic (Anenburg et al., 2021; Yaxley et al., 2022).
86 Different processes have been proposed for their formation, although there is a consensus that they originate
87 from primary fusion processes derived from a carbonated mantle (Kamenetsky et al., 2021). For the specific
88 case of the oceanic carbonatites, this debate is even more lively. Doucelance et al. (2010) suggested a
89 shallow origin from low-degree partial melting at the base of the oceanic lithosphere. Other authors have
90 proposed the involvement of unmixing process linking to alkaline magma suites (Weidendorfer et al.,
91 2016), the action of hydrothermal fluids of marine origin enriched in Ca that would have serpentinized the
92 mantle (Park and Rye, 2013) or even the contribution of recycled marine carbonates through subduction or
93 assimilated in shallow magma chambers (Démeny et al., 1998; Hoernle et al., 2002; Doucelance et al.,
94 2014).

95 The present work concentrates on the mineralogical and geochemical study of carbonatites and associated
96 alkaline igneous rocks, along with their weathering products, in three different sectors in the western region
97 of Fuerteventura (Canary Islands, Spain; Figure 1). The primary goal of this research is to conduct an initial
98 evaluation of these materials, which are genetically associated with a volcanic island linked to an oceanic
99 intraplate magmatism. This assessment aims to enhance our understanding of REE accumulation while
100 appraising the potential of this peculiar geological environment as a non-conventional source of REE.

101

102 **2 Geological setting**

103 **2.1 The Canary Island Seamount Province**

104 The Canary Islands archipelago, located between 27°N and 30°N of latitude, is part of the Canary Island
105 Seamount Province (CISP). This volcanic region forms a band of approximately 1300 km in length and
106 350 km in width, running parallel to the African continental margin. Within the CISP, there are over 100
107 seamounts and up to 8 emerged islands: El Hierro, La Palma, La Gomera, Tenerife, Gran Canaria,
108 Lanzarote, Fuerteventura and Savage islands (Courtillot et al., 2003; Schmincke and Sumita, 2010; van den
109 Bogaard, 2013). Based on magnetic anomaly measurements and dating of both emerged and submarine
110 igneous materials, volcanic activity in the CISP spans more than 142 Ma, from the Early Cretaceous to the
111 present day (Frisch, 2012; van den Bogaard, 2013; Longpré and Felpeto, 2021).

112 **2.2 Fuerteventura Island**

113 Fuerteventura, the easternmost island of the Canarian archipelago, along with Lanzarote, forms the
114 emergent crest of the Eastern Canarian Volcanic Ridge, which is located approximately 100 km offshore
115 from the Moroccan coast (Figure 1). Fuerteventura is the oldest island in the archipelago, with its initial
116 stages of formation linked with submarine volcanic activity, dating to the Oligocene (~34 Ma). The first
117 episodes of subaerial volcanism occurred around ~23 Ma (Coello, 1992; Ancochea et al., 1996; Pérez-
118 Torrado et al., 2023).

119 Fuerteventura is characterized by the occurrence of three distinct main geological units, arranged in order
120 from oldest to youngest: the Fuerteventura basal complex (FBC), the Miocene subaerial volcanic units, and
121 the Pliocene-Quaternary volcano-sedimentary facies (Fúster et al., 1968; Le Bas et al., 1986; Muñoz et al.,
122 2005; Gutiérrez et al., 2006; Troll and Carracedo, 2016).

123

124 **2.2.1 The Fuerteventura basal complex**

125 The FBC unit mainly outcrops in the western part of the island (Figure 1). Two different groups of
126 lithofacies may be distinguished: (1) Early Jurassic to Late Cretaceous oceanic crust materials (Steiner et
127 al., 1998), constituted by mid-ocean ridge basalts and oceanic sediments; (2) Oligocene submarine and
128 transitional volcanic rocks associated with plutonic bodies and dyke swarms (Feraud et al., 1985; Hobson
129 et al., 1998; Gutiérrez et al., 2006). In this second group, a set of lithologies can be distinguished related to
130 an ultra-alkaline-carbonatitic magmatic pulse that occurred ~25 Ma (Le Bas, 1981; Barrera et al., 1986;
131 Balogh et al., 1999). Additionally, alkaline ultramafic, mafic and felsic plutonic rocks such as wehrlites,
132 pyroxenites, gabbros and syenites intruded the previously existing Oligocene materials, forming distinctive
133 ring complexes (Muñoz et al., 2005). These magmatic rocks, predominantly of Oligocene age, have been
134 interpreted as episodes of submarine and transitional growth in Fuerteventura (Le Bas et al., 1986; Gutiérrez
135 et al., 2006).

136 In general, outcrops related with the FBC intrusive assemblage exhibit significant variations and four
137 distinct morphologies and characteristic textures can be identified (Fúster et al., 1968; Barrera et al., 1986;
138 Le Bas et al., 1986; Fernández et al., 1997; Mangas et al., 1992, 1994, 1997; Ahijado 1999; Ancochea et
139 al., 2004; Ahijado et al., 2005; Muñoz et al., 2005):

- 140 (1) Basaltic, alkaline and carbonatitic dykes and veins of meter-scale, decimeter-scale, and
141 centimeter-scale, that are randomly distributed, resulting in a chaotic arrangement (Figure 2a, b).
142 Related to the carbonatite veins and dikes, an intense fenitization may occur.
- 143 (2) Shear zones (Fernández et al., 1997), characterized by gradual or diffuse boundaries, which
144 display assimilation structures between different rock bodies, along with the presence of
145 mylonites, and brecciated textures resulting from deformation (Figure 2c).
- 146 (3) Pegmatitic textures developed within certain rock bodies, often containing centimeter-sized
147 crystals of rock-forming minerals (Figure 2d).
- 148 (4) Contact metamorphism and metasomatism, as well as skarn zones that occur in deformed or
149 undeformed carbonatites, influenced by subsequent hydrothermal fluid circulation (Ahijado et al.,
150 2005; Casillas et al., 2008, 2011).

151

152 In addition, during Miocene magmatic pulses, alkaline plutons were formed in the central-western part of
153 Fuerteventura Island north of the locality of Pájara (sector 2, Figure 1). These intrusions constitute typical
154 ring complexes of alkaline magmatic rocks, including nepheline syenites, syenites, and trachytes (Muñoz,
155 1969). They are regarded as the most recent rocks in the FBC (Figure 1) and have been dated using the K-
156 Ar method, yielding an approximate age of 20.6 ± 1.7 Ma (Le Bas et al., 1986; Holloway and Bussy, 2008).

157

158 **2.2.2 Miocene subaerial volcanic unit**

159 During the Miocene, Fuerteventura witnessed the formation of up to three volcanic edifices (Figure 1;
160 Coello et al., 1992; Ancochea et al., 1996). The northern volcanic structure, referred to as the Tetir edifice,
161 experienced two volcanic construction phases between 22 and 12.8 Ma (Balcells et al., 1994). These
162 episodes involved the eruption of basalts, picritic basalts, oceanic basalts, trachybasalts and trachytes. In
163 the central part of the island, the Gran Tarajal edifice developed three different construction phases
164 spanning from 22.5 to 14.5 Ma (Balcells et al., 1994). On the Jandía Peninsula, in the southern part of the
165 island, a volcanic edifice comprising both basaltic and trachybasaltic materials emerged. It formed three
166 successive construction episodes occurring between 20.7 and 14.2 Ma ago (Balcells et al., 1994). Based on
167 their mineralogical and petrological features, the lithologies comprising this unit have not been considered
168 as potentially containing significant concentrations of REEs. Therefore, they have not been included in the
169 evaluation conducted in the present study.

170

171 **2.2.3 Pliocene and Quaternary volcano-sedimentary facies**

172 After the subaerial volcanic activity during the Miocene, a period of volcanic quiescence ensued, leading
173 to the erosion of the previously formed volcanic edifices. Subsequently, during the Pliocene (between 5.3
174 and 2.6 Ma), a phase of magmatic rejuvenation began, characterized by scattered Strombolian eruptions
175 (Figure 1). Concurrently, various sedimentary formations emerged across the entire island, including littoral
176 and shallow-water marine deposits, as well as aeolian, colluvial, and alluvial subaerial sediments and
177 paleosols from the Pliocene to the Quaternary (Fúster et al., 1968; Zazo et al., 2002; Ancochea et al., 2004).
178 The soils on Fuerteventura are predominantly classified as eutric cambisols and lithosols-vitric andosols,
179 according to the FAO/UNESCO (1970) nomenclature. However, the current arid and deforested conditions
180 have led to extensive erosion of the weathered rock profiles present in different areas of the island. Edaphic
181 calcretes are abundant in Fuerteventura (Alonso-Zarza and Silva, 2002; Huerta et al., 2015), with their
182 primary source of calcium believed to be the Pliocene paleodunes formed by calcarenites, rather than the
183 parent igneous rock itself (Chiquet et al., 1999; Huerta et al., 2015; Alonso-Zarza et al., 2020). Interestingly,
184 the aeolian dust deposits predominantly originate from the Sahara Desert (Goudie and Middleton, 2001;
185 Menéndez et al., 2007; Scheuven et al., 2013).

186

187

188

189

190 **3 Materials and Methods**

191 **3.1 Sampling**

192 Alkaline magmatic rocks and especially carbonatites are considered potential targets for the exploration of
193 rare earth elements (Goodenough et al., 2016; Balaram et al., 2019; Anenburg et al., 2021; Beland and
194 Jones, 2021). In Fuerteventura, these types of lithologies are found in two distinct geological areas: the
195 Oligocene (sectors 1 and 3; Figure 1) and the Miocene lithologies related with the FBC (sector 2, Figure
196 1).

197 Considering that weathering profiles may concentrate REE in larger quantities than primary bedrocks (Bao
198 and Zhao, 2008; Menéndez et al., 2019, Braga and Biondi, 2023; Chandler et al., 2024), these lithological
199 formations were included in the present evaluation study and sampling was conducted on a selection of six

200 different profiles: (1) Agua Salada ravine (sector 1) and (2) Aulagar ravine (sector 3), developed on
201 carbonatites, (3) the FV-30 road, (4) Las Peñitas quarry, (5) Palomares ravine and (6) the Pájara profiles,
202 on syenite bedrock (Figure 1; Table S1).

203 Accordingly, a systematic sampling campaign was conducted in three different sectors of Fuerteventura,
204 targeting alkaline and carbonatitic igneous rocks and their associated weathering products. The specific
205 locations of these predetermined sectors are outlined in Figure 1. As a result, a set of 29 representative
206 samples of potentially REE-enriched magmatic rocks, along with 21 samples of associated weathering
207 products, were collected for further analysis and evaluation (Table S1). For the weathering products, we
208 conducted six sampling profiles (labelled A to F; Figure 1) at various suitable points to compare the
209 mineralogical and geochemical changes resulting from weathering of the primary magmatic rocks.

210

211 **3.2 Petrographic and mineralogical studies**

212 Selected samples of magmatic rocks were prepared in thin sections for textural and mineralogical analysis
213 at the Laboratory of Geological and Paleontological Preparation of the Natural Sciences Museum of
214 Barcelona (LPGiP-MCNB; Barcelona, Spain). A representative subset of these samples was also examined
215 using a JEOL JSM-7100 field emission scanning electron microscope (FE-SEM) at the Scientific and
216 Technological Centers of the Universitat de Barcelona (CCiTUB). The FE-SEM system is equipped with
217 an INCA Pentaflex EDS (energy dispersive spectroscopy) detector (Oxford Instruments, England), which
218 allowed for the acquisition of semi-quantitative analyses of mineral phases. The general operating
219 conditions for the FE-SEM were a 15-20 kV accelerating voltage and a 5 nA beam current.

220 To achieve accurate and precise mineralogical identification and characterization of the weathering
221 magmatic rocks and calcretes, X-ray powder diffraction (XRPD) measurements were performed using a
222 PANalytical Empyrean powder diffractometer equipped with a PIXcel1D Medipix 3 detector at the
223 Integrated XRD Service of the General Research Support Service of La Laguna University, Spain. The
224 diffractometer employed incident Cu K α radiation at 45 kV and 40 mA, along with an RTMS (real-time
225 multiple strip) PIXcel1D detector with an amplitude of 3.3473° 2 θ . The diffraction patterns were obtained
226 by scanning random powders in the 2 θ range from 5° to 80°. Data sets were generated using a scan time of
227 57 seconds and a step size of 0.0263° (2 θ), with a 1/16° divergence slit. Mineral identification and semi-
228 quantitative results were obtained using the PANalytical's HighScore Plus search-match software (v. 4.5)
229 with a PDF+ database.

230

231 **3.3 Geochemical analyses**

232 The major elements composition of carbonates from carbonatites was studied using an electron probe
233 microanalyzer (EPMA) system. The EPMA analyses were conducted on a JEOL JXA-8230 electron
234 microprobe, equipped with five wavelength-dispersive spectrometers and a silicon-drift detector EDS,
235 located at the CCiTUB. The spot mode was employed for the analyses and the electron column was set to
236 an accelerating voltage of 15 kV and a beam current of 10 nA. Standard counting times of 10 seconds were
237 used, along with a focused beam, to achieve the highest possible lateral resolution. The analytical standards
238 employed during the analysis process were: celestine (PETJ, Sr K_α) wollastonite (PETL, Ca K_α), periclase
239 (TAPH, Mg K_α), hematite (LiFH, Fe K_α), rhodonite (LiFH, Mn K_α) and albite (TAPH, Na K_α).

240 Bulk-rock geochemical data of major and trace element composition were obtained by X-ray fluorescence
241 (XRF) and inductive coupled plasma (ICP)-emission spectrometry. The samples were prepared by lithium
242 metaborate/tetraborate fusion and nitric acid digestion at the ACTLABS Activation Laboratories Ltd.
243 (Ancaster, Canada).

244

245 **4 Results**

246 **4.1 Petrography and mineralogy**

247 **4.1.1 Alkaline magmatic rocks and carbonatites**

248 The primary lithologies under study, consist of Oligocene (~25 Ma) alkaline igneous and carbonatitic rocks,
249 as well as Miocene alkaline lithologies (K–Ar age of 20.6±1.7 Ma; Le Bas et al., 1986), that form part of
250 the FBC. Their outcrops extend across kilometer-scale areas but exhibit high heterogeneity at a detailed
251 level due to the occurrence of numerous small intrusions, ranging in size from metric to decimetric
252 dimensions (Figs. 2a, b).

253 At a mineralogical level, separation of the different types of alkaline rocks found in the FBC is complex
254 because these lithologies are intimately associated and infiltrate diffusely, leading to the formation of hybrid
255 intrusions. The materials with the most mafic composition correspond to pyroxenites and melteigites, and
256 their formation is associated with the earliest magmatic fractions. However, these are commonly spatially
257 associated with more differentiated rocks, mainly ijolites, nepheline syenites, and syenites. All these
258 lithologies have a relatively simple mineralogy, characterized by varying proportions of nepheline (10-30%
259 modal) and potassium feldspar (50-80% modal), associated with aegirine-augite and biotite (10-30%

260 modal). A set of accessory minerals with varying proportions (always less than 5% modal) also occur,
261 including ilmenite, titanite, zircon, and fluorapatite.

262 At a textural level, the alkaline series lithologies of the FBC present granular textures with millimeter-sized
263 euhedral grains. However, in some of the intrusions in sectors 2 and 3, pegmatitic syenites-ijolites were
264 detected with centimeter-sized grains characterized by the presence of large aegirine-augite crystals.

265 Some of the intrusions described in the three sectors show aphanitic textures caused by faster cooling,
266 resulting in rocks with similar mineralogy but extrusive-type textural characteristics. Therefore, due to their
267 textural features, some dikes and apophyses, although mineralogically equivalent, should be classified as
268 trachytes and phonolites.

269 Carbonatitic intrusions commonly co-occur with the alkaline rocks, sharing similar morphology, textures,
270 and spatial distribution within the outcrops (Figure 2e). Furthermore, alkaline and/or carbonatitic intrusions
271 can be occasionally associated with mafic intrusions, primarily pyroxenites and alkaline gabbros. In
272 addition, a subsequent set of mafic dikes with basaltic composition overlaps the previous intrusive bodies
273 (Figs. 2a, b).

274 All carbonatites described in different outcrops from sectors 1 and 3 are predominantly composed of calcite
275 (95% modal) and can thus be classified as calciocarbonatites (Le Maitre, 2005). None of the studied samples
276 shows the occurrence of ferromagnesian carbonates such as ankerite, dolomite, and/or siderite, as well as
277 REE carbonates. Texturally, calcite occurs as euhedral crystals ranging in size from millimetres to
278 centimetres, often recrystallized and exhibiting polysynthetic twinning. In some cases, a secondary micritic
279 calcite matrix is present, filling interstitial spaces and fractures.

280 The major element composition of calcite is relatively consistent across all the carbonatite samples.
281 Notably, there are significant contents of SrO, with values of up to 5.43 wt%, while REEs are absent from
282 the carbonate composition (Table S2).

283 The accessory mineralogy (~5% modal) comprises disseminated phases within the calcium carbonate.
284 Among them, the occurrence of minerals from the spinel group, including magnetite (Figure 3a), and
285 primarily jacobsonite, occurring as subhedral crystals of up to 50 μm (Figure 3b). Another characteristic
286 mineral is perovskite, occurring as subhedral crystals of up to 100 μm . These grains are remarkable for
287 their significant Nb contents, as described in other carbonatitic localities worldwide (Torró et al., 2012).
288 Britholite also occurs as subhedral crystals of up to 100 μm (Figure 3b). This primary britholite contains
289 significant LREE content (Figure 4), and its alteration leads to the formation of secondary REE-enriched

290 phosphates, mainly monazite-Nd (Figure 3c), which also contains substantial amounts of La and Ce (Figure
291 4). REEs, in addition to occurring in primary britholite and secondary monazite, were also detected in tiny
292 pyrochlore grains, heterogeneously disseminated in the calcite groundmass (Figure 3b). In some cases,
293 pyrochlore forms euhedral crystals of up to 20 μm , also included in calcite (Figure 3d). This pyrochlore
294 shows slight zoning towards plumbopyrochlore (Christy and Atencio, 2013), with significant enrichment
295 in Pb observed at grain borders (Figure 3d).

296 Carbonatites can be affected by certain contact metamorphism, especially in sectors 1 and 3 (Figure 1) and
297 may exhibit a slightly different mineralogy from the one described thus far. This is characterized by the
298 occurrence of skarn-type metamorphic minerals, formed due to the interaction between carbonatites and
299 spatially associated silica-rich rocks. Among these minerals, there are subhedral crystals of andradite, up
300 to 30 μm in size, implanted in a matrix of secondary calcite and phlogopite, exhibiting pronounced zoning
301 with kerimasite cores (Figure 3e). In these areas, the occurrence of REE mineralizations associated with
302 allanite (Figure 3f) is also typical. Allanite occurs as granular aggregates associated with hydrothermal
303 secondary sulfates, primarily baryte (Figure 3f), but occasionally celestine (Figure 3c).

304 This particular mineralogy, typically associated with skarn formations, emerges from the interaction
305 between a carbonatite intrusion and surrounding silicate rocks, in contrast to the typical process. It has
306 recently gained attention from several researchers in various carbonatite locations worldwide, who have
307 coined the term antiskarn to describe it (Anenburg and Mavrogenes, 2018; Yaxley et al., 2022).

308

309 **4.1.2 Weathering products**

310 In certain areas within the three studied sectors (Figure 1), there is evidence of the development of
311 characteristic shallow geological formations consistently associated with weathering, which affect the
312 outlined magmatic lithologies (Figs. 5, 6). These geological products were studied through the analysis of
313 six alteration profiles, developed on carbonatites (Agua Salada and Aulagar) and syenites (Palomares
314 ravine, FV-30 road, Las Peñitas quarry, and Pájara) (Figure 1).

315 The carbonatite-calcrete sections generally consist of centimetre-scale calcrete veins injected into the
316 bedrock, seemingly without any apparent connection to the current upward lithosol (Figure 5). In general,
317 the development of soils or weathering products was not detected on carbonatites in any of the studied
318 sectors of the FBC.

319 Weathering products developed on syenite bedrock are generally more abundant, and the corresponding
320 alteration profiles are better preserved than in carbonatites. The cambic B horizon displays reddish to
321 yellowish colorations (5YR6/6), with a thickness of up to 20-30 cm. Additionally, it is common to find BC
322 horizons instead of B horizons, while the C horizon is well-developed, reaching a 30-40 cm thickness at
323 certain levels of the profile (Figure 6). Furthermore, except for the Las Peñitas profile (E profile, Figure 1),
324 centimetre-scale calcrete bands (Bk; Jahn et al., 2006) were also detected in deeper layers across all the
325 studied profiles.

326 In terms of mineralogical composition, carbonatite profiles exhibit significant changes due to weathering.
327 In general, weathering processes lead to a reduction in calcite, the disappearance of fluorapatite, and the
328 formation of secondary minerals like palygorskite (Figure 7). The contribution from lateral slope movement
329 is also evident through the presence of residual plagioclase and clinopyroxene.

330 In the case of syenite weathering profiles, illite/chlorite and kaolinite are the predominant secondary
331 products, followed by muscovite and palygorskite (Figure 7). Other minerals such as quartz were also
332 detected, even in the C horizons.

333

334 **4.2 Bulk-rock and mineral geochemistry**

335 Chemical analysis of the major, minor and trace elements were carried out in order to evaluate the
336 geochemical features and the distribution of REEs, on 25 representative samples of igneous rocks from the
337 FBC, including trachytes, phonolites, syenites, ijolites and carbonatites (Table S3). In addition, we also
338 analysed 21 samples of weathering products (Table S4).

339 The total REY (REEs plus yttrium) content in the FBC igneous rocks exhibits widespread and significant
340 enrichment in comparison to the average crustal values (~125 ppm, Rudnick and Gao, 2014). Notably, the
341 extrusive and magmatic alkaline lithologies (trachytes and phonolites as well as syenites and ijolites) show
342 variable REY values ranging between about 230 and 1,400 ppm (Table S3). In contrast, the carbonatitic
343 rocks exhibit REY content more than ten times greater than the alkaline lithologies, with specific samples
344 reaching maximum values of up to about 10,300 ppm, as evidenced in sample 85a sourced from a
345 carbonatite outcrop in sector 1 (Table S3).

346 The weathered magmatic rocks, though moderately significant in REY content relative to the average
347 crustal values (Table S4), still exhibit slightly lower levels compared to the content observed in the
348 associated alkaline and carbonatitic protoliths (Table S3). A contrasting pattern emerges in the calcretes,

349 where REY values experience a sharp reduction, presenting virtually negligible values ranging between 20
350 and 72 ppm REY. These levels are significantly below the average Earth's crust values (Rudnick and Gao,
351 2014) and are markedly lower than those observed in both the alkaline lithologies and, particularly, the
352 carbonatites of the FBC.

353 REE normalized diagrams further underscore this distribution, portraying elevated content in the
354 carbonatites, followed by the alkaline rocks (Figure 8a). Meanwhile, the weathered magmatic rocks and
355 calcretes (Figure 8b) display significantly lower values. All studied lithologies exhibit clear negative
356 patterns, indicative of enrichment in LREEs relative to HREEs. Notably, carbonatites and alkaline rocks
357 (Figure 8a) exhibit a flattening of these negative patterns in the final segment, indicating a certain degree
358 of HREE enrichment.

359 The FCB carbonatites exhibit a depletion in some critical elements commonly associated with this lithology
360 such as Nb or Ta (Table S3). Negative anomalies of both Nb and Ta are clearly observed in the multi-
361 element diagrams of carbonatite samples (Figure 9a). However, given the presence of pyrochlore in the
362 carbonatites, these anomalies in Nb and Ta are likely not indicative. We interpret that the low concentrations
363 of these elements could be attributed to an analytical artifact that would underestimate the contents of High
364 Field Strength Elements (HFSE) due to the challenge of pyrochlore dissolution in the analytical digestion
365 protocols employed. These protocols have been primarily devised to assess the contents of REEs rather
366 than HFSE. Additionally, alkaline rock patterns also show a distinctive negative anomaly in Sr (Figure 9b).
367 As for the weathering products, their contents of other minor elements do not indicate significant
368 concentrations of metals or critical elements like Nb or Ta (Table S4). The multi-element diagrams for the
369 calcretes exhibit a negative Ta anomaly (Figure 9c), while the patterns of weathered magmatic rocks do not
370 reveal notable anomalies in any group of elements (Figure 9d).

371 A specific geochemical study of REE distribution in the six studied weathering profiles was also conducted
372 (Figure 10). The main objective was to evaluate the geochemical interactions between the protolith and the
373 related weathering lithologies, with the aim of detecting potential REE enrichments or depletions caused
374 by weathering processes.

375 In the exchange patterns of calcretes spatially associated with carbonatitic protoliths, as analyzed in the
376 Agua Salada and Aulagar ravine profiles (Figs. 10A, B), REE concentrations are two orders of magnitude
377 lower than in the carbonatite (Figure 10A), as also previously determined from the REE diagrams (Figure
378 8). Notably, it was found that the REE concentration is directly proportional to the distance from the

379 protolith (Figure 10B), and calcrete samples with the highest REE concentrations (sample 14; Figure 10)
380 were found in closer proximity to the primary carbonatites than more REE depleted samples (samples 15
381 and 18; Figure 10B). In addition, although the values of all elements are depleted in the calcrete patterns,
382 there is a greater depression in LREE than in HREE relative to the protolith, resulting in typically positive
383 patterns, except for sample 76 from the Agua Salada ravine, where a clear inverse trend is observed (Figure
384 10A).

385 In general, the diagrams in Figure 10 show that weathering products on syenites exhibit enrichment relative
386 to the protolith (green areas in Figs. 10C, D, E). However, calcrete samples, whether derived from
387 carbonatites or syenites, consistently show depletions compared to the protolith contents (reddish areas in
388 Figs. 10C, D, F). The diagrams corresponding to the weathering products generated on syenites exhibit
389 similar morphologies (Figs. 10C, D, E, F). Overall, these lithologies are characterized by enrichment in
390 REEs relative to the protolith as well as V-shaped patterns, featured by the presence of a negative anomaly
391 in Eu, which is also reported in all C and B horizons developed on syenites, except sample 61 (Figure 10C),
392 and is likely related to plagioclase crystallization.

393

394 **5 Discussion**

395 **5.1 REE evaluation of the FBC magmatic rocks**

396 The FBC magmatic rocks, in the three study sectors, encompass alkaline lithologies (trachytes, phonolites,
397 syenites, melteigites, and ijolites) as well as carbonatites. Regarding the group of alkaline rocks, the
398 detected REE content varies between 214 and 1,330 ppm (Table S3), significantly higher than the average
399 concentration determined in the Earth's crust (~125 ppm, Rudnick and Gao, 2014). However, this finding
400 is not surprising, and the observed values in Fuerteventura are not anomalous, as these types of lithologies
401 typically exhibit REE concentrations within this range (Dostal, 2017). Therefore, the measured REE
402 concentrations are neither significant nor sufficiently elevated to hypothetically consider these lithologies
403 as a potential non-conventional deposit of these critical elements in the FBC.

404 On the other hand, FBC carbonatites present significantly higher values in terms of REE content. In the
405 studied carbonatite samples from sectors 1 and 3 (carbonatites do not outcrop in sector 2), REE content
406 ranges between about 1300 ppm and 10,300 ppm. The latter value corresponds to the richest REE-detected
407 sample in the entire FBC, which is located in the Agua Salada ravine area of sector 1 (Table S3; Figure 1).

408 The reported REE content values in the FBC carbonatites are similar to the general average concentrations
409 found in other locations worldwide where carbonatites are exploited for REE extraction. This is the case,
410 for example, of Bayan Obo, the largest REE mine in the world in terms of reserves and production (Lai et
411 al., 2015; Liu et al., 2018). In this locality, high-grade carbonatites exhibit average concentrations of 2880
412 ppm (Wu et al., 2008; Smith et al., 2015, 2016), which are equivalent to those measured in some of the
413 samples from Fuerteventura. It should be noted that low-grade carbonatite ore from Bayan Obo presents
414 extremely high values in comparison to the FBC, with REE concentrations reaching 30,750 ppm (Chao et
415 al., 1997; Smith et al., 2016).

416 Another significant example is the Mountain Pass carbonatite in California, USA, regarded as the largest
417 REE mine in the American continent, intermittently in operation for REE extraction since 1954 (Olson et
418 al., 1954; Haxel, 2005). In this REE deposit, average value across the whole complex are around 2580 ppm
419 (Castor et al., 2008; Mariano and Mariano, 2012; Smith et al., 2016), also in line with REE concentrations
420 detected in the present study for the FBC carbonatites.

421 This comparative analysis can also be carried out using normalized REE values (Figure 11). In this regard,
422 FBC carbonatites are significantly depleted in LREE compared to those from Bayan Obo (Yang et al.,
423 2019) and Mountain Pass (Castor et al., 2008), although they show similar values to other REE deposits
424 associated with carbonatites, such as those in Ashram, Canada (Beland and Jones, 2021) and Bear Lodge,
425 USA (Moore et al., 2015; Smith et al., 2016; Figure 11). However, the pattern of the Fuerteventura
426 carbonatites exhibits a slightly less pronounced slope, indicating a higher relative content of HREE, which
427 are considered the materials with the highest risk of supply among all the CRMs defined by the EC
428 (European Commission, 2023a). In fact, in the FBC carbonatites, the normalized HREE values are
429 equivalent to those reported in the primary carbonatitic rocks from the deposits of Bayan Obo (China) and
430 Mountain Pass (USA) (Figure 11). The relative significant HREE content reported in FBC carbonatites
431 holds particular significance for several economic and technological reasons. The use of HREEs, such as
432 Yb, Er, and Tm, is of particular interest in cutting-edge photonic and nanotechnology applications.

433 At the mineralogical level, it was observed that, in the FBC carbonatites, the main REE-hosting minerals
434 are accessory phases; primarily minerals from the pyrochlore group, found as disseminated euhedral micro-
435 crystals implanted in primary calcite (Figs. 3b, d). Another REE-bearing mineral in the FBC carbonatites
436 is britholite, which exhibits significant LREE content. However, this mineral is commonly altered to

437 monazite (Figs. 3c, 4), interpreted as a secondary phase but also a carrier of these critical elements (Chen
438 et al., 2017).

439 Another noteworthy aspect is the lack of REE fluorcarbonates like bastnäsite $\text{REE}(\text{CO}_3)\text{F}$, parisite
440 $\text{Ca}(\text{REE})_2(\text{CO}_3)_3\text{F}_2$, synchysite $\text{Ca}(\text{REE})(\text{CO}_3)_2\text{F}$ or huanghoite $\text{Ba}(\text{REE})(\text{CO}_3)_2\text{F}$. They do not occur in the
441 FBC, as they do in other REE deposits associated with, for example, the Bayan Obo carbonatite or the
442 Sulphide Queen carbonatite from Mountain Pass (Castor et al., 2008; Smith et al., 2015, 2016). This point
443 is crucial for a future hypothetical evaluation of the FBC carbonatites, as the processing of oxides and
444 phosphates for REE extraction is a much more complex and expensive treatment process than for REE-
445 bearing carbonates (McNulty et al., 2022).

446

447 **5.2 REE evaluation of associated weathering products**

448 The weathering materials developed on magmatic rocks, also analysed for their REE concentrations,
449 constitute the remnants of soils that were interpreted as developed under wetter conditions during a humid
450 phase of the oxygen isotope stage 2, spanning from 29 to 20 thousand years BP (Huerta et al., 2016). This
451 period aligns with the last glacial maximum, marked by heightened humidity in the Canary Islands,
452 resulting in slope erosion and the formation of talus flatiron (Gutiérrez-Elorza et al., 2013). Over time, these
453 materials have undergone substantial volume reduction due to human-driven deforestation and erosion,
454 primarily before the 15th century (Machado-Yanes, 1996). Notably, topography plays an essential role in
455 the distribution of these weathering profiles and influences specific physical attributes such as slope
456 (FAO/UNESCO, 1974).

457 The studied weathering products developed on syenite rocks (profiles C, D, E, F; Figs. 1, 7) are classified
458 by FAO/UNESCO (1974) as eutric cambisols, reflecting a Mediterranean climate condition. Indeed, on the
459 African continent, which is adjacent to the Canary Islands, eutric cambisols are primarily found within the
460 tropical subhumid zone, gradually transitioning into the semi-arid zone (FAO/UNESCO, 1974). These
461 syenite weathering profiles exhibit better-preserved characteristics and a more significant extent compared
462 to those studied in carbonatites (profiles A and B; Figs. 1, 7). In general, intensive weathering plays a
463 crucial role in the formation of REE deposits, as these elements tend to be concentrated in such geological
464 formations compared to others leached during the weathering process. This phenomenon is exemplified in
465 several locations worldwide, where REE deposits associated with weathering products occur: for instance,
466 Bear Lodge in the USA (Andersen et al., 2017), Chuktukon and Tomtor in Russia (Kravchenko and

467 Pokrovsky, 1995; Kravchenko et al., 2003; Chebotarev et al., 2017), Las Mercedes in the Dominican
468 Republic (Torró et al., 2017), Araxá in Brazil (Braga and Biondi, 2023), and Mount Weld in Australia
469 (Zhukova et al., 2021; Chandler et al., 2024), among many others. However, the weathering processes on
470 Fuerteventura are characterized by fluctuating climatic conditions and intense erosion in the context of a
471 typical Mediterranean climate, which is in turn characterized by drier conditions and a lower propensity for
472 intense weathering compared to tropical climates. The weathering processes on Fuerteventura do not
473 therefore typically lead to the development of laterites and mature weathering profiles, since these
474 conditions do not favor the formation and subsequent preservation of these products, particularly within
475 the carbonatite bedrock areas. Consequently, this constraint substantially reduces the capacity of the FBC
476 to potentially contain economically valuable REE concentrations within the associated weathering
477 products.

478

479 **5.3 Fuerteventura carbonatites as potential REE source**

480 Based on the mineralogical and geochemical data, it can be concluded that, among the lithologies studied
481 in the FBC, only the carbonatites are favorable targets for further characterization and evaluation of their
482 potential economic viability as an REE source. Therefore, the primary alkaline rocks, as well as the entire
483 suite of corresponding secondary weathering products, can be ruled out.

484 The geochemical data obtained from the oceanic carbonatites of Fuerteventura, exemplified in multielement
485 and REE diagrams (Figure 8), suggest a petrogenetic affinity with carbonatites associated with
486 intracontinental rift geological settings. This similarity has also been previously highlighted by other
487 authors such as Carnevale et al. (2021) who, based on stable isotope data ($\delta^{13}\text{C}$ and $\delta^{18}\text{C}$) and noble gases
488 isotopic composition (He, Ne, Ar), suggested that oceanic and continental carbonatites were comparable in
489 petrogenetic terms. Therefore, despite the lingering questions about the formation processes of oceanic
490 carbonatites, their assessment as a possible source of critical metals, especially REEs, should be fully
491 considered in the same way as their continental counterparts.

492 However, when considering a more detailed assessment of the sectors where the FBC carbonatites outcrop,
493 it is essential to note that the distribution of these outcrops and thus potential REE mineralization is not
494 straightforward. The carbonatite outcrops have a very limited surface distribution, in the order of meters
495 (Figure 2e), and exhibit complex structural features influenced by shear metamorphism (Figure 2c) and
496 overlapping episodes of intrusive activity that resulted in swarms of dikes with intricate distributions (Figs.

497 2a, b). Hence, these general features of the carbonatite outcrops make it imperative to validly estimate their
498 volume and to carry out more precise studies of their depth distribution, which likely involve drilling and
499 geophysical techniques. These prospective hypothetical findings would provide a deeper understanding of
500 the morphology and dimensions of the carbonatitic bodies, enhancing the ability to calculate resources and
501 reserves while refining the general metallogenic modeling.

502 However, it is important to highlight that any attempt to assess potential REE deposits linked to FBC
503 carbonatites must consider the irregular distribution of these mineralizations. In addition, it should also be
504 considered the existence of regulatory constraints that may stem from the allocation of land for strategic
505 military activities, as well as environmental considerations to safeguard natural and marine-coastal areas,
506 especially bearing in mind that Fuerteventura is a UNESCO biosphere reserve territory. This latter point is
507 particularly pertinent for a specific area within sector 3 (Figure 1). Therefore, any comprehensive analysis
508 of the potential of FBC carbonatites as REE sources must also factor in these potential restrictions tied to
509 land use regulations aimed at upholding the broader socio-economic, environmental, and societal interests
510 inherent to a distinctive site like the island of Fuerteventura.

511

512 **6 Conclusions**

513 A preliminary evaluation of rare earth element (REE) content was conducted through a mineralogical and
514 geochemical study of alkaline and carbonatitic igneous rocks within the Fuerteventura basal complex
515 (FBC), along with associated weathering products. Based on the gathered data and their corresponding
516 interpretations, our findings can be summarized as follows:

- 517 (i) The concentrations of REEs present in the alkaline and carbonatitic rocks of the FBC are
518 significant and exceed the average values attributed to the Earth's crust.
- 519 (ii) The weathering products developed on these magmatic rocks do not exhibit significant REE
520 enrichment.
- 521 (iii) Calcified horizons (Bk, calcretes), spatially related with carbonatites, have practically
522 negligible concentrations of REE elements. Colluvial processes may have influenced the
523 lateral transport and accumulation of REEs in Pleistocene-Holocene deposits distant from the
524 source area.
- 525 (iv) Among the magmatic rocks, carbonatites are the only lithology studied within the FBC with
526 a real potential to host REE mineral resources. The detected concentrations of REY in

527 carbonatites range up to about 10,300 ppm, which is a comparable concentration to other
528 locations hosting significant deposits of these critical elements worldwide.

529 (v) Within carbonatites, REEs are primarily hosted in two accessory mineral phases: (1) oxides
530 belonging to the pyrochlore group; and (2) phosphates. In this second group, primary phases
531 such as REE-bearing britholite can be distinguished, as well as monazite generated as a
532 secondary product from the britholite alteration.

533 (vi) Primary calcite in the Fuerteventura carbonatites is not the predominant host of REEs. It
534 displays a highly homogeneous composition with insignificant Fe-Mg content and negligible
535 REEs.

536 (vii) The carbonatites within the FBC could be considered potential REE resources associated with
537 a non-conventional geological setting. However, the complex structural features of the studied
538 FBC outcrops (deformation, metamorphism, swarms of dikes from different intrusive
539 pulses...) make it essential to conduct more detailed studies to quantify the real economic
540 possibilities of this lithology as an REE source.

541 (viii) All the studied sectors contain outcrops located in restricted areas due to environmental or
542 military use concerns. Any further detailed evaluation of the FBC carbonatites must take into
543 account the environmental, socio-economic, and geostrategic factors that will significantly
544 limit the real potential extension of REE deposits, considering a hypothetical exploitation.

545

546 **Acknowledgements**

547 This research was funded by the “Tierras Raras” project (SD-22/25) and the “MAGEC-REEmounts”
548 project (ProID-20211010027) of the Canarian Agency for Research, Innovation and Information Society
549 (ACIISI by its initials in Spanish) of the Canary Islands Government. Funding support was also provided
550 by the project “Materials for Advanced Energy Generation” (ENE2013-47826-C4-4-R), “3D Printed
551 Advanced Materials for Energy Applications” (ENE2016-74889-C4-2-R) and “Estudio de los procesos
552 magmáticos, tectónicos y sedimentarios involucrados en el crecimiento temprano de edificios volcánicos
553 oceánicos en ambiente de intraplaca” (CGL2016-75062-P), all funded by the Government of Spain. The
554 collection of samples in specific protected areas required authorization from the Fuerteventura Island
555 Government. We appreciate the cooperation and assistance provided by the Spanish Army, especially by
556 the soldier Liberto Yeray Puga Acosta, who facilitated our access to the Pájara CMT restricted military

557 area to carry out sampling. We also thank Gerard Lucena from the LPGiP-MCNB for his thorough work in
558 the elaboration of polished thin sections.

559

560 **Statements and Declarations**

561 **Data availability statement**

562 The authors confirm that the data supporting the findings of this study are available within the article and
563 its supplementary materials.

564

565 **Competing interests**

566 The authors declare no competing interests. The funders had no role in the design of the study, in the
567 collection of samples, the analyses, the interpretation of data, the writing of the manuscript nor the decision
568 to publish these results.

569 **Author contributions**

570 Conceptualization: MC, IM, LQ, JY, JM; fieldwork and sampling: MC, IM, LQ, JY, RC, AA, JM;
571 methodology: MC, IM, JY, JM; validation of results: MC, IM, LQ, JY, RC, JMR, JM; data curation: MC,
572 IM, JM; writing-original draft preparation: MC, IM, JY, JM; writing-review editing: MC, IM, LQ, JY, RC,
573 JMR, JM; supervision: IM, JY, JM; project administration: JMR, JM; funding acquisition: IM, JY, RC,
574 JMR, JM.

575

576 **Additional information**

577 Supplementary tables are available in the online version at [https: XXXXX](https://XXXXX)

578 **References**

- 579 Acosta-Mora, P., Domen, K., Hisatomi, T., Lyu, H., Méndez-Ramos, J., Ruiz-Morales, J. C., Khaidukov,
580 N. M.: “A bridge over troubled gaps”: up-conversion driven photocatalysis for hydrogen generation
581 and pollutant degradation by near-infrared excitation, *Chem. Commun*, 54, 1905–1908
582 <https://doi.org/10.1039/C7CC09774C>, 2018.
- 583 Aiglsperger, T., Proenza, J. A., Lewis, J. F., Labrador, M., Svojtka, M., Rojas-Purón, A., Longo, F.,
584 Āurišová, J.: Critical metals (REE, Sc, PGE) in Ni laterites from Cuba and the Dominican Republic,
585 *Ore Geol. Rev.*, 73, 127–147, <https://doi.org/10.1016/j.oregeorev.2015.10.010>, 2016.
- 586 Ahijado, A.: Las intrusiones plutónicas e hipoabisales del sector meridional del Complejo Basal de
587 Fuerteventura, Doctoral Thesis, Universidad Complutense de Madrid, 392 p., 1999.
- 588 Ahijado, A., Casillas, R., Nagy, G., Fernández, C.: Sr-rich minerals in a carbonatite skarn, Fuerteventura,
589 Canary Islands (Spain), *Mineralogy and Petrology*, 84, 107–127, <https://doi.org/10.1007/s00710-005-0074-8>, 2005.
- 591 Alonso, E., Sherman, A. M., Wallington, T. J., Everson, M. P., Field, F. R., Roth, R., Kirchain, R. E.:
592 Evaluating Rare Earth Element Availability: A Case with Revolutionary Demand from Clean
593 Technologies, *Environ. Sci. Technol.*, 46, 3406–3414, <https://doi.org/10.1021/es203518d>, 2012.
- 594 Alonso-Zarza, A. M., Silva, P. G.: Quaternary laminar calcretes with bee nests evidences of small-scale
595 climatic fluctuations, Eastern Canary Islands, Spain, *Palaeogeogr. Palaeoclimatol. Palaeoecol.*, 178,
596 119–135, [https://doi.org/10.1016/S0031-0182\(01\)00405-9](https://doi.org/10.1016/S0031-0182(01)00405-9), 2002.
- 597 Alonso-Zarza, A. M., Rodríguez-Berriguete, Á., Casado, A. I., Martín-Pérez, A., Martín-García, R.,
598 Menéndez, I., Mangas, J.: Unravelling calcrete environmental controls in volcanic islands, Gran
599 Canaria Island, Spain, *Palaeogeogr. Palaeoclimatol. Palaeoecol.*, 554, 109797,
600 <https://doi.org/10.1016/j.palaeo.2020.109797>, 2020.
- 601 Ancochea, E., Brändle, J. L., Cubas, C. R., Hernán, F., Huertas, M. J.: Volcanic complexes in the eastern
602 ridge of the Canary Islands: the Miocene activity of the Island of Fuerteventura, *Journal of*
603 *Volcanology and Geothermal Research*, 70, 183–204, [https://doi.org/10.1016/0377-0273\(95\)00051-](https://doi.org/10.1016/0377-0273(95)00051-8)
604 [8](https://doi.org/10.1016/0377-0273(95)00051-8), 1996.
- 605 Ancochea, E., Barrera, J. L., Bellido, F.: Canarias y el vulcanismo neógeno peninsular. *Geología de España*,
606 635-682. In: Aparicio, A., Hernán, F., Cubas, C. R., Araña, V., 2003, Fuentes mantélicas y evolución
607 del vulcanismo canario, *Estudios Geológicos*, 59, 5–13, <https://doi.org/10.3989/egeol.03591-477>,
608 2004.
- 609 Andersen, A. K., Clark, J. G., Larson, P. B., Donovan, J. J.: REE fractionation, mineral speciation, and
610 supergene enrichment of the Bear Lodge carbonatites, Wyoming, USA, *Ore Geology Reviews*, 89,
611 780–807, <https://doi.org/10.1016/j.oregeorev.2017.06.025>, 2017.
- 612 Anenburg, M., Mavrogenes, J.A., Carbonatitic versus hydrothermal origin for fluorapatite REE-Th
613 deposits: experimental study of REE transport and crustal “antiskarn” metasomatism, *American*
614 *Journal of Science*, 318, 335–366, <https://doi.org/10.2475/03.2018.03>, 2018.
- 615 Anenburg, M., Broom-Fendley, S., Chen, W.: Formation of Rare Earth Deposits in Carbonatites, *Elements*,
616 17, 327–332, <https://doi.org/10.2138/gselements.17.5.327>, 2021.

617 Balcells, R., Barrera, J. L., Gómez, J. A., Cueto, L. A., Ancochea, E., Huertas, M. J., Ibarrola, E., Snelling,
618 N.: Edades radiométricas en la Serie Miocena de Fuerteventura (Islas Canarias), *Bol. Geol. Min.*, 35,
619 450–470, 1994.

620 Balaram, V.: Rare earth elements: A review of applications, occurrence, exploration, analysis, recycling,
621 and environmental impact, *Geoscience Frontiers*, 10, 1285–1303,
622 <https://doi.org/10.1016/j.gsf.2018.12.005>, 2019.

623 Balogh, K., Ahijado, A., Casillas, R., Fernández, C.: Contributions to the chronology of the Basal Complex
624 of Fuerteventura, Canary Islands, *Journal of Volcanology and Geothermal Research*, 90, 81–101,
625 [https://doi.org/10.1016/S0377-0273\(99\)00008-6](https://doi.org/10.1016/S0377-0273(99)00008-6), 1999.

626 Bao, Z., Zhao, Z.: Geochemistry of mineralization with exchangeable REY in the weathering crusts of
627 granitic rocks in South China, *Ore Geol. Rev.*, 33, 519–535,
628 <https://doi.org/10.1016/j.oregeorev.2007.03.005>, 2008.

629 Barrera, J. L., Fernández-Santín, S., Fúster, J. M., Ibarrola, E.: Ijolitas-Sienitas-Carbonatitas de los Macizos
630 del Norte de Fuerteventura, *Bol. Geol. Min.*, TXCII-IV, 309–321. ISSN 0366-0176, 1993.

631 Barteková, E., Kemp, R., National strategies for securing a stable supply of rare earths in different world
632 regions, *Resources Policy*, 49, 153–164, <https://doi.org/10.1016/j.resourpol.2016.05.003>, 2016.

633 Beland, C. M. J., William-Jones, A. E.: The mineralogical distribution of the REE in carbonatites: A
634 quantitative evaluation, *Chemical Geology*, 585, 120558,
635 <https://doi.org/10.1016/j.chemgeo.2021.120558>, 2021.

636 Berger, A., Janots, E., Gnos, E., Frei, R., Bernier, F., Rare earth element mineralogy and geochemistry in
637 a laterite profile from Madagascar. *Applied Geochemistry* 41, 218–228,
638 <https://doi.org/10.1016/j.apgeochem.2013.12.013>, 2014.

639 Borst, A. M., Smith, M. P., Finch, A. A., Estrade, G., Villanova-de-Benavent, C., Nason, P., Marquis, E.,
640 Horsburgh, N. J., Goodenough, K. M., Xu, C., Kynický, J., Geraki, K.: Adsorption of rare earth
641 elements in regolith-hosted clay deposits, *Nat. Commun.*, 11, 4386, <https://doi.org/10.1038/s41467-020-17801-5>, 2020.

643 Braga, J. M., Biondi, J. C.: Geology, geochemistry, and mineralogy of saprolite and regolith ores with Nb,
644 P, Ba, REEs (+ Fe) in mineral deposits from the Araxá alkali-carbonatitic complex, Minas Gerais
645 state, Brazil, *Journal of South American Earth Sciences*, 125, 104311,
646 <https://doi.org/10.1016/j.jsames.2023.104311>, 2023.

647 Braun, J. J., Pagel, M., Herbillin, A., Rosin, C.: Mobilization and redistribution of REEs and thorium in a
648 syenitic lateritic profile: A mass balance study, *Geochem. Cosmochim. Acta*, 57, 4419–4434.
649 [https://doi.org/10.1016/0016-7037\(93\)90492-F](https://doi.org/10.1016/0016-7037(93)90492-F), 1993.

650 Carnevale, G., Caracausi, A., Correale, A., Italiano, L., Rotolo, S.G., An Overview of the Geochemical
651 Characteristics of Oceanic Carbonatites: New Insights from Fuerteventura Carbonatites (Canary
652 Islands), *Minerals*, 11, 203. <https://doi.org/10.3390/min11020203>, 2021.

653 Casillas, R., Nagy, G., Demény, A., Ahijado, A., Fernández, C.: Cuspidine–niocalite–baghdadite solid
654 solutions in the metacarbonatites of the Basal Complex of Fuerteventura (Canary Islands). *Lithos*
655 105:25–41. <https://doi.org/10.1016/j.lithos.2008.02.003>, 2008.

656 Casillas, R., Démeny, A., Nagy, G., Ahijado, A., Fernández, C.: Metacarbonatites in the Basal Complex of
657 Fuerteventura (Canary Islands). The role of fluid/rock interactions during contact metamorphism and
658 anatexis, *Lithos*, 125, 503–520, <https://doi.org/10.1016/j.lithos.2011.03.007>, 2011.

659 Castor, S. B.: The Mountain Pass rare-earth carbonatite and associated ultrapotassic rocks, California, The
660 Canadian Mineralogist, 46, 779–806, <https://doi.org/10.3749/canmin.46.4.779>, 2008.

661 Chakhmouradian, A. R., Wall, F.: Rare Earth Elements: Minerals, Mines, Magnets (and More), *Elements*,
662 8, 333–340, <https://doi.org/10.2113/gselements.8.5.333>, 2012.

663 Chao, E. C. T., Back, J. M., Minkin, J. A., Tatsumoto, M., Wang, J., Conrad, J. E., McKee, E. H., Hou, Z.
664 L., Meng, Q. R., Huang, S. G.: The sedimentary carbonate-hosted giant Bayan Obo REE-Fe-Nb ore
665 deposit of Inner Mongolia, China: a corner stone example for giant polymetallic ore deposits of
666 hydrothermal origin, *USGS Bulletin*, 2143, 65, <https://doi.org/10.3133/b2143>, 1997.

667 Chandler, R., Bhat, G., Mavrogenes, J., Knell, B., David, R., Leggo, T.: The primary geology of the
668 Paleoproterozoic Mt Weld carbonatite complex, Western Australia, *Journal of Petrology*, 65, 2,
669 <https://doi.org/10.1093/petrology/egae007>, 2024.

670 Charalampides, G., Vatalis, K., Baklavariadis, A., Benetis, N. P.: Rare Earth Elements: Industrial
671 Applications and Economic Dependency of Europe, *Procedia Economics and Finance*, 24, 126–135,
672 [https://doi.org/10.1016/S2212-5671\(15\)00630-9](https://doi.org/10.1016/S2212-5671(15)00630-9), 2015.

673 Chebotarev, D. A., Doroshkevich, A., Klemd, R., Karmanov, N.: Evolution of Nb- mineralization in the
674 Chuktukon carbonatite massif, Chadobets upland (Krasnoyarsk Territory, Russia), *Periodico di*
675 *Mineralogia*, 86, 99–118, <https://doi.org/10.2451/2017PM733>, 2017.

676 Chen, W., Honghui, H., Bai, T., Jiang, S.: Geochemistry of Monazite within Carbonatite Related REE
677 Deposits, *Resources*, 6, 51, <https://doi.org/10.3390/resources6040051>, 2017.

678 Chiquet, A., Michard, A., Nahon, D., Hamelin, B.: Atmospheric input vs in situ weathering in the genesis
679 of calcretes: an Sr isotope study at Gálvez (Central Spain), *Geochim. Cosmochim. Acta*, 63, 311–323,
680 [https://doi.org/10.1016/S0016-7037\(98\)00271-3](https://doi.org/10.1016/S0016-7037(98)00271-3), 1999.

681 Christy, A. G., Atencio, D.: Clarification of status of species in the pyrochlore supergroup, *Mineralogical*
682 *Magazine*, 77, 13–20, <https://doi.org/10.1180/minmag.2013.077.1.02>, 2013.

683 Christy, A.G., Pekov, I.V., Krivovichev, S.G., The Distinctive Mineralogy of Carbonatites, *Elements*, 17,
684 333–338, <https://doi.org/10.2138/gselements.17.5.333>, 2021.

685 Coello, J., Cantagrel, J. M., Hernán, F., Fúster, J. M., Ibarrola, E., Ancochea, E., Casquet, C., Jamond, C.,
686 Díaz-de-Terán, J. R., Cendrero, A.: Evolution of the Eastern volcanic ridge of Canary Islands based
687 on new K-Ar data, *Journal of Volcanology and Geothermal Research*, 53, 251–274,
688 [https://doi.org/10.1016/0377-0273\(92\)90085-R](https://doi.org/10.1016/0377-0273(92)90085-R), 1992.

689 Connelly, N. G., Hartshorn, R. M., Damhus, T., Hutton, A. T.: Nomenclature of Inorganic Chemistry
690 IUPAC Recommendations 2005, RSC Publishing, Cambridge, ISBN-0-85404-438-8, 2005.

691 Courtillot, V., Davaille, A., Besse, J., Stock, J.: Three distinct types of hotspots in the Earth's mantle, *Earth*
692 *Planet. Sci. Letters*, 205, 295–308, [https://doi.org/10.1016/S0012-821X\(02\)01048-8](https://doi.org/10.1016/S0012-821X(02)01048-8), 2003.

693 De Ignacio, C., Muñoz, M., Sagredo, J., Carbonatites and associated nephelinites from São Vicente, Cape
694 Verde Islands, *Min., Mag.*, 76, 311–355, doi:10.1180/minmag.2012.076.2.05, 2012.

695 Demény, A., Ahijado, A., Casillas, R., Vennemann, T.W., Crustal contamination and fluid/rock interaction
696 in the carbonatites of Fuerteventura (Canary Islands, Spain): A C, O, H isotope study, *Lithos*, 44, 101–
697 115, [https://doi.org/10.1016/S0024-4937\(98\)00050-4](https://doi.org/10.1016/S0024-4937(98)00050-4), 1998.

698 Dostal, J.: Rare Earth Element Deposits of Alkaline Igneous Rocks, *Resources*, 6, 34–46,
699 <https://doi.org/10.3390/resources6030034>, 2017.

700 Doucelance, R., Hammouda, T., Moreira, M., Martins, J.C., Geochemical constraints on depth of origin of
701 oceanic carbonatites: The Cape Verde case, *Geochim. Cosmochim. Acta*, 74, 7261–7282,
702 <https://doi.org/10.1016/j.gca.2010.09.024>, 2010.

703 Doucelance, R., Bellot, N., Boyet, M., Hammouda, T., Bosq, C., What coupled cerium and neodymium
704 isotopes tell us about the deep source of oceanic carbonatites, *Earth Planet. Sci. Lett.*, 407, 175–186,
705 <https://doi.org/10.1016/j.epsl.2014.09.042>, 2014.

706 European Commission: European Green Deal, [https://commission.europa.eu/strategy-and-](https://commission.europa.eu/strategy-and-policy/priorities-2019-2024/european-green-deal_en)
707 [policy/priorities-2019-2024/european-green-deal_en](https://commission.europa.eu/strategy-and-policy/priorities-2019-2024/european-green-deal_en), 2019.

708 European Commission: Study on the Critical Raw Materials for the EU 2023 – Final Report,
709 <https://op.europa.eu/en/publication-detail/-/publication/57318397-fdd4-11ed-a05c-01aa75ed71a1> -
710 <https://doi.org/10.32873/725585>, 2023a.

711 European Commission, Regulation of the European Parliament and of the Council establishing a framework
712 for ensuring a secure and sustainable supply of critical raw materials and amending Regulations (EU)
713 168/2013, (EU) 2018/858, 2018/1724 and (EU) 2019/1020, [https://eur-lex.europa.eu/legal-](https://eur-lex.europa.eu/legal-content/EN/TXT/?uri=CELEX%3A52023PC0160)
714 [content/EN/TXT/?uri=CELEX%3A52023PC0160](https://eur-lex.europa.eu/legal-content/EN/TXT/?uri=CELEX%3A52023PC0160), 2023b.

715 FAO/UNESCO: Soil Map of the World Project 1:5000000, Chart VII, [https://www.fao.org/soils-](https://www.fao.org/soils-portal/data-hub/soil-maps-and-databases/faounesco-soil-map-of-the-world/en/)
716 [portal/data-hub/soil-maps-and-databases/faounesco-soil-map-of-the-world/en/](https://www.fao.org/soils-portal/data-hub/soil-maps-and-databases/faounesco-soil-map-of-the-world/en/), 1974.

717 Feraud, G., Giannerini, G., Campredon, R., Stillman, C.J.: Geochronology of some canarian dike swarms:
718 contribution to the volcano-tectonic evolution of the archipelago, *J. Volcanol. Geotherm. Res.*, 25,
719 29–52, [https://doi.org/10.1016/0377-0273\(85\)90003-4](https://doi.org/10.1016/0377-0273(85)90003-4), 1985.

720 Fernández, C., Casillas, R., Ahijado, A., Perelló, V., Hernández-Pacheco, A.: Shear zones as a result of
721 intraplate tectonics in oceanic crust: the example of the Basal Complex of Fuerteventura (Canary
722 Islands), *Jour. Struct. Geol.*, 19, 41–57, [https://doi.org/10.1016/S0191-8141\(96\)00074-0](https://doi.org/10.1016/S0191-8141(96)00074-0), 1997.

723 Frisch, T.: In: Schmincke, H. U., Sumita, M.: Geological evolution of the Canary Islands: a young volcanic
724 archipelago adjacent to the old African continent, *Bull. Volcanol.*, 74, 1255–1256,
725 <https://doi.org/10.1007/s00445-012-0605-1>, 2012.

726 Fúster, J. M., Cendrero, A., Gastesi, P., Ibarrola, E., López-Ruiz, J.: Geología y volcanología de las Islas
727 Canarias- Fuerteventura, Instituto “Lucas Mallada”, Consejo Superior de Investigaciones Científicas,
728 Madrid. 239 pp, 1968.

729 Goodenough, K. M., Schilling, J., Jonsson, E., Kalvig, P., Charles, N., Tuduri, J., Deady, E. A., Sadeghi,
730 M., Schiellerup, H., Müller, A., Bertrand, G., Arvanitidis, N., Eliopoulos, D. G., Shaw, R. A., Thrane,
731 K., Keulen, N.: Europe’s rare earth element resource potential: An overview of REE metallogenetic
732 provinces and their geodynamic setting, *Ore Geol. Rev.*, 72, 838–856,
733 <https://doi.org/10.1016/j.oregeorev.2015.09.019>, 2016.

734 Goudie, A. S., Middleton, N. J.: Saharan dust storms: nature and consequences, *Earth Sci. Rev.*, 56, 179–
735 204, [https://doi.org/10.1016/S0012-8252\(01\)00067-8](https://doi.org/10.1016/S0012-8252(01)00067-8), 2001.

736 Graedel, T. E., Harper, E. M., Nassar, N. T., Reck, B. K.: Criticality of metals and metalloids, *Proceedings*
737 *of the National Academy of Sciences*, 112 4257–4262, <https://doi.org/10.1073/pnas.1500415112>,
738 2015.

739 Gutiérrez, M., Casillas, R., Fernández, C., Balogh, K., Ahijado, A., Castillo, C., Colmenero, J. R., García-
740 Navarro, E.: The submarine volcanic succession of the basal complex of Fuerteventura, Canary
741 Islands: A model of submarine growth and emergence of tectonic volcanic islands, *Bulletin of the*
742 *Geological Society of America*, 118, 785–804, <https://doi.org/10.1130/B25821.1>, 2006.

743 Gutiérrez-Elorza, M., Lucha, P., Gracia, F. J., Desir, G., Marín, C., Petit-Maire, N.: Palaeoclimatic
744 considerations of talus flatirons and aeolian deposits in Northern Fuerteventura volcanic island
745 (Canary Islands, Spain), *Geomorphology*, 197, 1–9, <https://doi.org/10.1016/j.geomorph.2011.09.020>,
746 2013.

747 Haxel, G. B.: Ultrapotassic mafic dikes and rare earth element- and barium-rich carbonatite at Mountain
748 Pass, Mojave Desert, southern California: summary and field trip localities, *U.S. Geol. Surv. Open-*
749 *File Rep.*, 1219. <http://pubs.usgs.gov/of/2005/1219/>, 2005.

750 Hobson, A., Bussy, F., Hernández, J.: Shallow-level migmatization of gabbros in a metamorphic contact
751 aureole, Fuerteventura Basal Complex, Canary Islands, *Journal of Petrology*, 39, 1025–1037,
752 <https://doi.org/10.1093/petroj/39.5.1025>, 1998.

753 Hoernle, K., Tilton, G., Le Bas, M.J., Duggen, S., Garbe-Schönberg, D., Geochemistry of oceanic
754 carbonatites compared with continental carbonatites: Mantle recycling of oceanic crustal carbonate,
755 *Contrib. Mineral. Petrol.*, 142, 520–542, <https://doi.org/10.1007/s004100100308>, 2002.

756 Holloway, M. I., Bussy, F.: Trace element distribution among rock-forming minerals from metamorphosed
757 to partially molten basic igneous rocks in a contact aureole (Fuerteventura, Canaries), *Lithos*, 102,
758 616–639, <https://doi.org/10.1016/j.lithos.2007.07.026>, 2008.

759 Huerta, P., Rodríguez-Berriguete, A., Martín-García, R., Martín-Pérez, A., La-Iglesia-Fernández, A.,
760 Alonso-Zarza, A.: The role of climate and eolian dust input in calcrete formation in volcanic islands
761 (Lanzarote and Fuerteventura, Spain), *Palaeogeogr. Palaeoclimatol. Palaeoecol.*, 417, 66–79,
762 <https://doi.org/10.1016/j.palaeo.2014.10.008>, 2015.

763 Humphreys-Williams, E.R., Zahirovic, S.: Carbonatites and Global Tectonics, *Elements*, 17, 339–344,
764 <https://doi.org/10.2138/gselements.17.5.339>, 2021.

765 Jahn, R., Blume, H. P., Asio, V. B., Spaargaren, O., Schad, P.: Guidelines for soil description, FAO, Rome
766 97 p, <https://www.fao.org/3/a0541e/a0541e.pdf>, 2006.

767 Jyothi, R. K., Thenepalli, T., Ahn, J. W., Parhi, P. K., Chung, K. W., Lee, J. Y.: Review of rare earth
768 elements recovery from secondary resources for clean energy technologies: grand opportunities to
769 create wealth from waste, *J. Clean. Prod.*, 267, 122048, <https://doi.org/10.1016/j.jclepro.2020.122048>,
770 2020.

771 Kamenetsky, V.S., Doroshkevich, A.G., Elliot, H.A.L., Zaitsev, A.N., Carbonatites: Contrasting, Complex,
772 and Controversial, *Elements*, 17, 307–314, <https://doi.org/10.2138/gselements.17.5.307>, 2021.

773 Kravchenko, S. M., Pokrovsky, B. G.: The Tomtor alkaline ultrabasic massif and related REE-Nb deposits,
774 northern Siberia, *Economic Geology*, 90, 676–689, <https://doi.org/10.2113/gsecongeo.90.3.676>,
775 1995.

776 Kravchenko, S. M., Czamanske, G., Fedorenko, V. A.: Geochemistry of carbonatites of the Tomtor massif,
777 *Geochem. Int.*, 41, 545–558, ISSN: 0016-7029, 2003.

778 Lai, X., Yang, X., Santosh, M., Liu, Y., Ling, M.: New data of the Bayan Obo Fe-REE-Nb deposit, Inner
779 Mongolia: Implications for ore genesis, *Precambrian Research*, 263, 108–122,
780 <https://doi.org/10.1016/j.precamres.2015.03.013>, 2015.

781 Le Bas, M. J.: The pyroxenite-ijolite-carbonatite intrusive igneous complexes of Fuerteventura, Canary
782 Islands, *J. Geol. Soc. London*, 138, 496, <https://doi.org/10.1144/gsjgs.138.4.0493>, 1981.

783 Le Bas, M. J., Rex, D. C., Stillman, C. J.: The early magmatic chronology of Fuerteventura, *Geol. Mag.*,
784 123, 287–298, <https://doi.org/10.1017/S0016756800034762>, 1986.

785 Le Maitre, R. W., *Igneous Rocks: a Classification and Glossary of Terms*, Cambridge University Press,
786 Cambridge, U.K., 2002.

787 Le Maitre, R. W., Streckeisen, A., Zanettin, B., Le Bas, M. J., Bonin, B., Bateman, P., Bellieni, G., Dudek,
788 A., Efremova, S., Keller, J., Lameyre, J., Sabine, P. A., Schmid, R., Sorensen, H., Woolley, A. R.:
789 *Igneous Rocks: A Classification and Glossary of Terms*, 2nd Edition, Cambridge, UK, Cambridge
790 Univ. Press, ISBN: 9780521619486, 2005.

791 Liu, Y. L., Ling, M. X., Williams, I. S., Yang, X. Y., Wang, C. Y., Sun, W.: The formation of the giant
792 Bayan Obo REE-Nb-Fe deposit, North China, Mesoproterozoic carbonatite overprinted Paleozoic
793 dolomitization, *Ore Geology Reviews*, 92, 73–83, <https://doi.org/10.1016/j.oregeorev.2017.11.011>,
794 2018.

795 Long, K. R., Van Gosen, B. S., Foley, N. K., Cordier, D.: The principal rare earth elements deposits of the
796 United States: A summary of domestic deposits and a global perspective,
797 <https://pubs.usgs.gov/sir/2010/5220/>, 2010.

798 Longpré, M. A., Felpeto, A.: Historical volcanism in the Canary Islands; part 1: A review of precursory
799 and eruptive activity, eruption parameter estimates, and implications for hazard assessment, *Journal*
800 *of Volcanology and Geothermal Research*, 419, 107363,
801 <https://doi.org/10.1016/j.jvolgeores.2021.107363>, 2021.

802 Machado-Yanes, M. C.: Reconstrucción paleoecológica y etnoarqueológica por medio del análisis
803 antracológico. La Cueva de Villaverde, Fuerteventura, In: *Biogeografía Pleistocena-Holocena de la*
804 *Península Ibérica*, 261274, Ramil-Rego, P., Fernández-Rodríguez, C., Rodríguez-Gutián, M. (Eds.),
805 ISBN 84-453-1716-4, 261 p, 1996.

806 Mangas, J., Pérez-Torrado, F. J., Reguillón, R. M., Cabrera, M. C.: Prospección radiométrica en rocas
807 alcalinas y carbonatitas de la serie plutónica I de Fuerteventura (Islas Canarias). Resultados
808 preliminares e implicaciones metalogénicas, *Actas del III Congreso Geológico de España y VIII*
809 *Congreso Latinoamericano de Geología*. Salamanca, 3, 389–393, ISBN: 84-600-8114-1, 1992.

810 Mangas, J., Pérez-Torrado, F. J., Reguillón, R. M., Martín-Izard, A.: Mineralizaciones de tierras raras
811 ligadas a los complejos intrusivos alcalino-carbonatíticos de Fuerteventura (Islas Canarias), *Bol. Soc.*
812 *Esp. Min.*, 17, 212–213, 1994.

813 Mangas, J., Pérez-Torrado, F. J., Reguillón, R. M., Martín-Izard, A.: Rare earth minerals in carbonatites of
814 Basal Complex of Fuerteventura (Canary Islands, Spain), In: Mineral Deposit: Research and
815 Exploration, where do they meet? Ed. Balkema, Rotterdam, 475–478, ISBN-13: 978-9054108894,
816 1997.

817 Mariano, A. N., Mariano, Jr. A.: Rare earth mining and exploration in North America, *Elements*, 8, 369–
818 376, <https://doi.org/10.2113/gselements.8.5.369>, 2012.

819 Massari, S., Ruberti, M.: Rare earth elements as critical raw materials: Focus on international markets and
820 future strategies, *Resour. Policy*, 38, 36–43, <https://doi.org/10.1016/j.resourpol.2012.07.001>, 2013.

821 McDonough, W., Sun, W.: The composition of the Earth, *Chemical Geology*, 67, 1050–1056,
822 [https://doi.org/10.1016/0009-2541\(94\)00140-4](https://doi.org/10.1016/0009-2541(94)00140-4), 1995.

823 McNulty, T., Hazen, N., Park, S., Processing the ores of rare-earth elements, *MRS Bulletin*, 47, 258–266,
824 <https://doi.org/10.1557/s43577-022-00288-4>, 2022.

825 Méndez-Ramos, J., Acosta-Mora, P., Ruiz-Morales, J. C., Hernández, T., Morge, M. E., Esparza, P.:
826 Turning into the blue: materials for enhancing TiO₂ photocatalysis by up-conversion photonics, *RSC*
827 *Advances*, 3, 23028–23034, <https://doi.org/10.1039/C3RA44342F>, 2013.

828 Menéndez, I., Díaz-Hernández, J. L., Mangas, J., Alonso, I., Sánchez-Soto, P. J.: Airborne dust
829 accumulation and soil development in the North-East sector of Gran Canaria (Canary Islands, Spain),
830 *J. Arid Environ.*, 71, 57–81, <https://doi.org/10.1016/j.jaridenv.2007.03.011>, 2007.

831 Menéndez, I., Campeny, M., Quevedo-González, L., Mangas, J., Llovet, X., Tauler, E., Barrón, V., Torrent,
832 J., Méndez-Ramos, J.: Distribution of REE-bearing minerals in felsic magmatic rocks and paleosols
833 from Gran Canaria, Spain: Intraplate oceanic islands as a new example of potential, non-conventional
834 sources of rare-earth elements, *Journal of Geochemical Exploration*, 204, 270–288,
835 <https://doi.org/10.1016/j.gexplo.2019.06.007>, 2019.

836 Moore, M., Chakhmouradian, A., Mariano, A. N., Sidhu, R.: Evolution of Rare-earth Mineralization in the
837 Bear Lodge Carbonatite, In: *Ore Geology Reviews*, 64, Mineralogical and Isotopic Evidence,
838 Wyoming, 499, 521, <http://dx.doi.org/10.1016/j.oregeorev.2014.03.015>, 2015.

839 Mourão, C., Mata, J., Doucelance, R., Madeira, J., da Silveira, A.B., Silva, L.C., Moreira, M., Quaternary
840 extrusive calciocarbonatite volcanism on Brava Island (Cape Verde): A nephelinite-carbonatite
841 immiscibility product, *Journal of African Earth Sciences*, 56, 59–74,
842 <https://doi.org/10.1016/j.jafrearsci.2009.06.003>, 2010.

843 Muñoz, M.: Ring complexes of Pájara in Fuerteventura Island, *Bulletin Volcanologique*, 33, 840–861,
844 <https://doi.org/10.1007/BF02596753>, 1969.

845 Muñoz, M., Sagredo, J., de Ignacio, C., Fernández-Suárez, J., Jeffries, T. E.: New data (U-Pb, K-Ar) on the
846 geochronology of the alkaline-carbonatitic association of Fuerteventura, Canary Islands, Spain,
847 *Lithos*, 85, 140–153, <https://doi.org/10.1016/j.lithos.2005.03.024>, 2005.

848 Olson, J.C., Shawe, D. R., Pray, L.C., Sharp, W. N.: Rare-Earth Mineral Deposits of the Mountain Pass
849 District, San Bernardino County, California, *Science*, 119, 325–326,
850 <https://doi.org/10.1126/science.119.3088.325>, 1954.

851 Park, J., Rye, D.M., Broader Impacts of the Metasomatic Underplating Hypothesis, *Geochem. Geophys.*
852 *Geosyst.*, 20, 4180–4829, <https://doi.org/10.1029/2019GC008493>, 2019.

853 Pérez-Torrado, F. J., Carracedo, J. C., Guillou, H., Rodríguez-González, A., Fernández-Turiel, J. L.: Age,
854 duration, and spatial distribution of ocean shields and rejuvenated volcanism: Fuerteventura and
855 Lanzarote, Eastern Canaries, *Journal of the Geological Society of London*, 180,
856 <https://doi.org/10.1144/jgs2022-112>, 2023.

857 Pirajno, F., Yu, H.C.: The carbonatite story once more and associated REE mineral systems, *Gondwana*
858 *Research*, 107, 281–295. <https://doi.org/10.1016/j.gr.2022.03.006>, 2022.

859 Reinhardt, N., Proenza, J., Villanova-de-Benavent, C., Aiglsperger, T., Bover-Arnal, T., Torró, L., Salas,
860 R., Dziggel, A.: Geochemistry and Mineralogy of Rare Earth Elements (REE) in Bauxitic Ores of the
861 Catalan Coastal Range, NE Spain, *Minerals*, 8, 562, <https://doi.org/10.3390/min8120562>, 2018.

862 Rudnick, R.L., Gao, S.: Composition of the Continental Crust, In: Holland, H.H., Turekian, K.K. (editors):
863 *Treatise on Geochemistry*, 4, 1–51, <https://doi.org/10.1016/B978-0-08-095975-7.00301-6>, 2014.

864 Scheuvens, D., Schütz, L., Kandler, K., Ebert, M., Weinbruch, S.: Bulk composition of northern African
865 dust and its source sediments—a compilation, *Earth Sci. Rev.*, 116, 170–194,
866 <https://doi.org/10.1016/j.earscirev.2012.08.005>, 2013.

867 Schmincke, H., Sumita, M.: Geological evolution of the Canary Islands: a young volcanic archipelago adjacent
868 to the old African Continent, Ed. Görres, Koblenz, 200 p, ISBN: 978-3-86972-005-0, 2010.

869 Smith, M. P., Campbell, L. S., Kynicky, J.: A review of the genesis of the world class Bayan Obo Fe-REE-Nb
870 deposits, Inner Mongolia, China: multistage processes and outstanding questions, *Ore Geology Reviews*,
871 64, 459–476, <https://doi.org/10.1016/j.oregeorev.2014.03.007>, 2015.

872 Smith, M. P., Moore, K., Kavcsánzski, D., Finch, A. A., Kynicky, J., Wall, F.: From mantle to critical zone:
873 A review of large and giant-sized deposits of the rare earth elements, *Geoscience Frontiers*, 7, 315–334,
874 <https://doi.org/10.1016/j.gsf.2015.12.006>, 2016.

875 Steiner, C., Hobson, A., Favre, P., Stampfli, G. M.: Early Jurassic sea-floor spreading in the central Atlantic
876 — the Jurassic sequence of Fuerteventura (Canary Islands), *Geological Society of American Bulletin*,
877 110, 1304–1317, [https://doi.org/10.1130/0016-7606\(1998\)110<1304:MSOFCI>2.3.CO;2](https://doi.org/10.1130/0016-7606(1998)110<1304:MSOFCI>2.3.CO;2), 1998.

878 Torró, L., Proenza, J. A., Aiglsperger, T., Bover-Arnal, T., Villanova-de-Benavent, C., Rodríguez-García,
879 D., Ramírez, A., Rodríguez, J., Mosquea, L.A., Salas, R.: Geological, geochemical and mineralogical
880 characteristics of REE-bearing Las Mercedes bauxite deposit, Dominican Republic, *Ore Geol. Rev.*,
881 89, 114–131, <https://doi.org/10.1016/j.oregeorev.2017.06.017>, 2017.

882 Torró, L., Villanova, C., Castillo, M., Campeny, M., Gonçalves, A. O., Melgarejo, J. C.: Niobium and rare
883 earth minerals from the Virulundo carbonatite, Namibe, Angola, *Mineralogical Magazine*, 76, 393–
884 409, <https://doi.org/10.1180/minmag.2012.076.2.08>, 2012.

885 Troll, V., Carracedo, J. C.: The Geology of Fuerteventura, In: Troll, V., Carracedo, J. C., Weismaier, S.
886 (eds), *The Geology of Canary Islands*, Elsevier, 531–582. [http://dx.doi.org/10.1016/B978-0-12-](http://dx.doi.org/10.1016/B978-0-12-809663-5.00008-6)
887 [809663-5.00008-6](http://dx.doi.org/10.1016/B978-0-12-809663-5.00008-6), 2016.

888 van den Bogaard, P.: The origin of the Canary Island Seamount Province - New ages of old seamounts,
889 *Scientific Reports*, 3, 2107. <https://doi.org/10.1038/srep02107>, 2013.

890 Wang, Q., Deng, J., Liu, X., Zhang, Q., Sun, S., Jiang, C., Zhou, F.: Discovery of the REE minerals and its
891 geological significance in the Quyang bauxite deposit, West Guangxi, China, *J. Asian Earth Sci.*, 39,
892 701–712, <https://doi.org/10.1016/j.jseaes.2010.05.005>, 2010.

893 Wang, X., Jiao, Y., Du, Y., Ling, W., Wu, L., Cui, T., Zhou, Q., Jin, Z., Lei, Z., Wen, S.: REE mobility
894 and Ce anomaly in bauxite deposit of WZD area, Northern Guizhou, China, *J. Geochem Explor.*, 133,
895 103–117, <https://doi.org/10.1016/j.gexplo.2013.08.009>, 2013.

896 Wang, Z.Y., Fan, H.R., Zhou, L., Yang, K.F., She, H.D., Carbonatite-related REE deposits: An
897 overview, *Minerals*, 10, 965. <https://doi.org/10.3390/min10110965>, 2020.

898 Warr, L. N.: IMA–CNMNC approved mineral symbols, *Mineralogical Magazine*, 85, 291–
899 320, <https://doi.org/10.1180/mgm.2021.43>, 2021.

900 Weidendorfer, D., Schmidt, M.W., Mattsson, H.B.: Fractional crystallization of Si-undersaturated alkaline
901 magmas leading to unmixing of carbonatites on Brava Island (Cape Verde) and a general model of
902 carbonatite genesis in alkaline magma suites, *Contributions to Mineralogy and Petrology*, 171, 43,
903 <https://doi.org/10.1007/s00410-016-1249-5>, 2016.

904 Weng, Z., Jowitt, S.M., Mudd, G.M., Haque, N.: A Detailed Assessment of Global Rare Earth Element
905 Resources: Opportunities and Challenges, *Economic Geology*, 110, 1925–1952,
906 <https://doi.org/10.2113/econgeo.110.8.192>, 2015.

907 Wondraczek, L., Tyystjärvi, E., Méndez-Ramos, J., Müller, F. A., Zhang, Q.: Shifting the Sun: Solar
908 Spectral Conversion and Extrinsic Sensitization in Natural and Artificial Photosynthesis, *Advanced
909 Science*, 2, 1500218, <https://doi.org/10.1002/advs.201500218>, 2015.

910 Woolley, A.R., Kjarsgaard, B.A. (2008): Carbonatites of the world: map and database. *Mineralogical
911 Magazine* 71, 718.

912 Wu, C.: Bayan Obo Controversy: Carbonatites versus Iron Oxide-Cu-Au-(REE-U), *Resource Geology*, 58,
913 348–354, <https://doi.org/10.1111/j.1751-3928.2008.00069.x>, 2008.

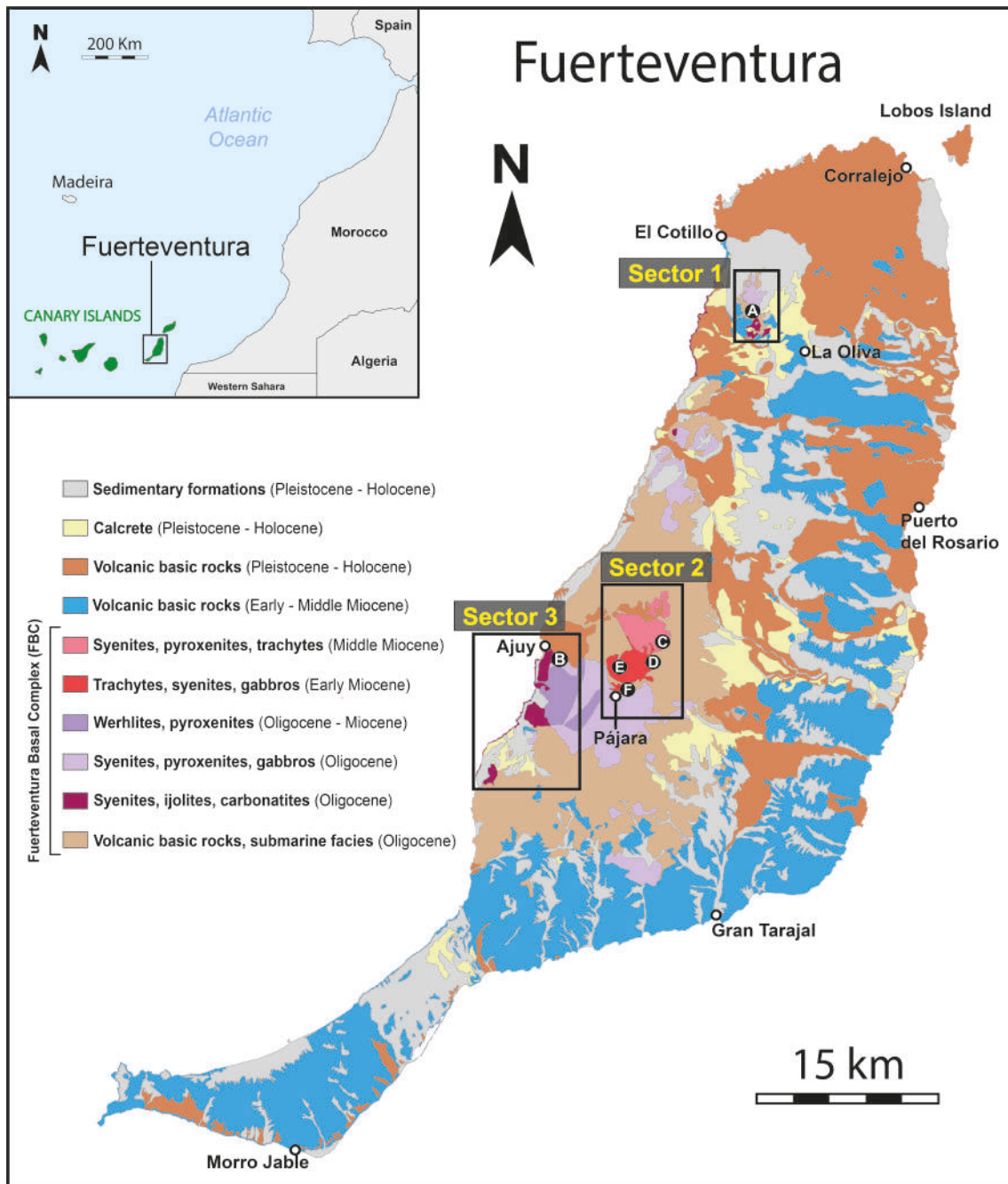
914 Yang, K., Fan, H., Pirajno, F., Li, X.: The bayan Obo (China) giant REE accumulation conundrum
915 elucidated by intense magmatic differentiation of carbonatite, *Geology*, 47, 1198–1202,
916 <https://doi.org/10.1130/G46674.1>, 2019.

917 Yaxley, G.M., Anenburg, M., Tappe, S., Decree, S., Guzmics, T.: Carbonatites: Classification, Sources,
918 Evolution, and Emplacement, *Annual Reviews on Earth and Planetary Sciences*, 50, 261–293,
919 <https://doi.org/10.1146/annurev-earth-032320-104243>, 2022.

920 Zazo, C., Goy, J. L., Hillaire-Marcel, C., Gillot, P. Y., Soler, V., González, J. A., Dabrio, C. J., Ghaleb, B.:
921 Raised marine sequences of Lanzarote and Fuerteventura revisited –a reappraisal of relative sea-level
922 changes and vertical movements in the eastern Canary Islands during the Quaternary, *Quaternary
923 Science Reviews*, 21, 2019–2046, [https://doi.org/10.1016/S0277-3791\(02\)00009-4](https://doi.org/10.1016/S0277-3791(02)00009-4), 2002.

924 Zhukova, I. A., Stepanov, A. S., Jiang, S. Y., Murphy, D., Mavrogenes, J., Allen, C., Chen, W., Bottrill,
925 R.: Complex REE systematics of carbonatites and weathering products from uniquely rich Mount
926 Weld REE deposit, Western Australia, *Ore Geology Reviews*, 139, 104539,
927 <https://doi.org/10.1016/j.oregeorev.2021.104539>, 2021.

928



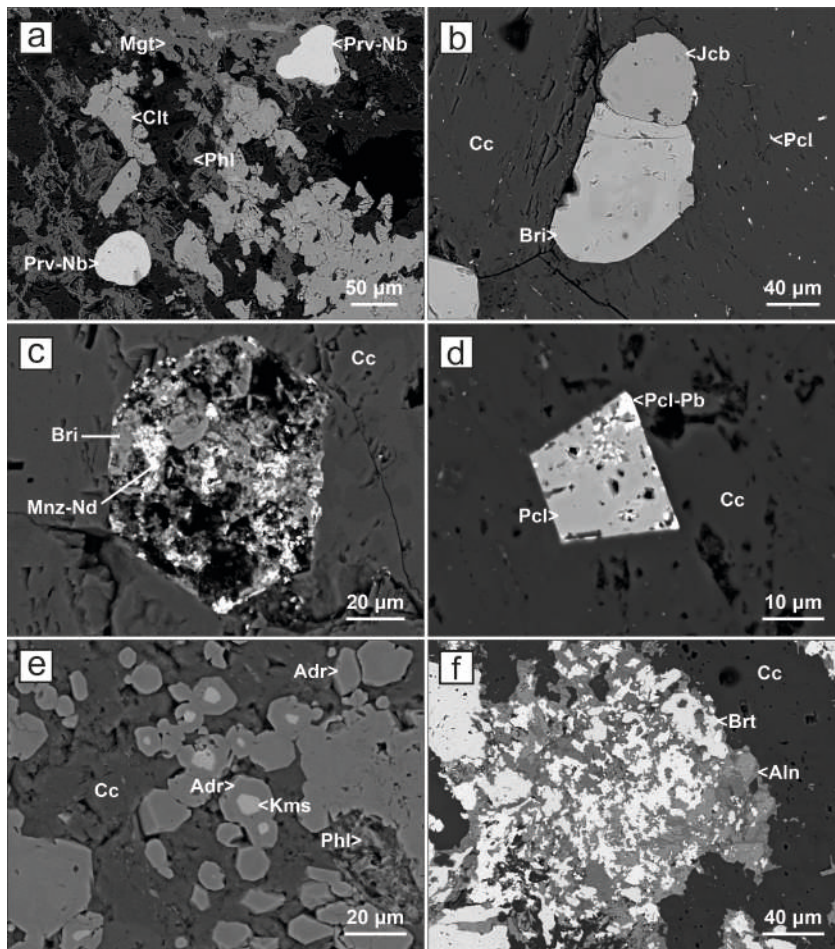
930
 931
 932
 933
 934
 935
 936
 937
 938

Figure 1: Simplified geological map of Fuerteventura Island (modified from Balcells et al., 2006) showing the location of the three study sectors for the assessment of REE content in the FBC. Additionally, the studied weathering profiles are also indicated, as: (A) Agua Salada ravine; (B) Aulagar ravine; (C) Palomares ravine; (D) FV-30 road; (E) Las Peñitas quarry; (F) Pájara.



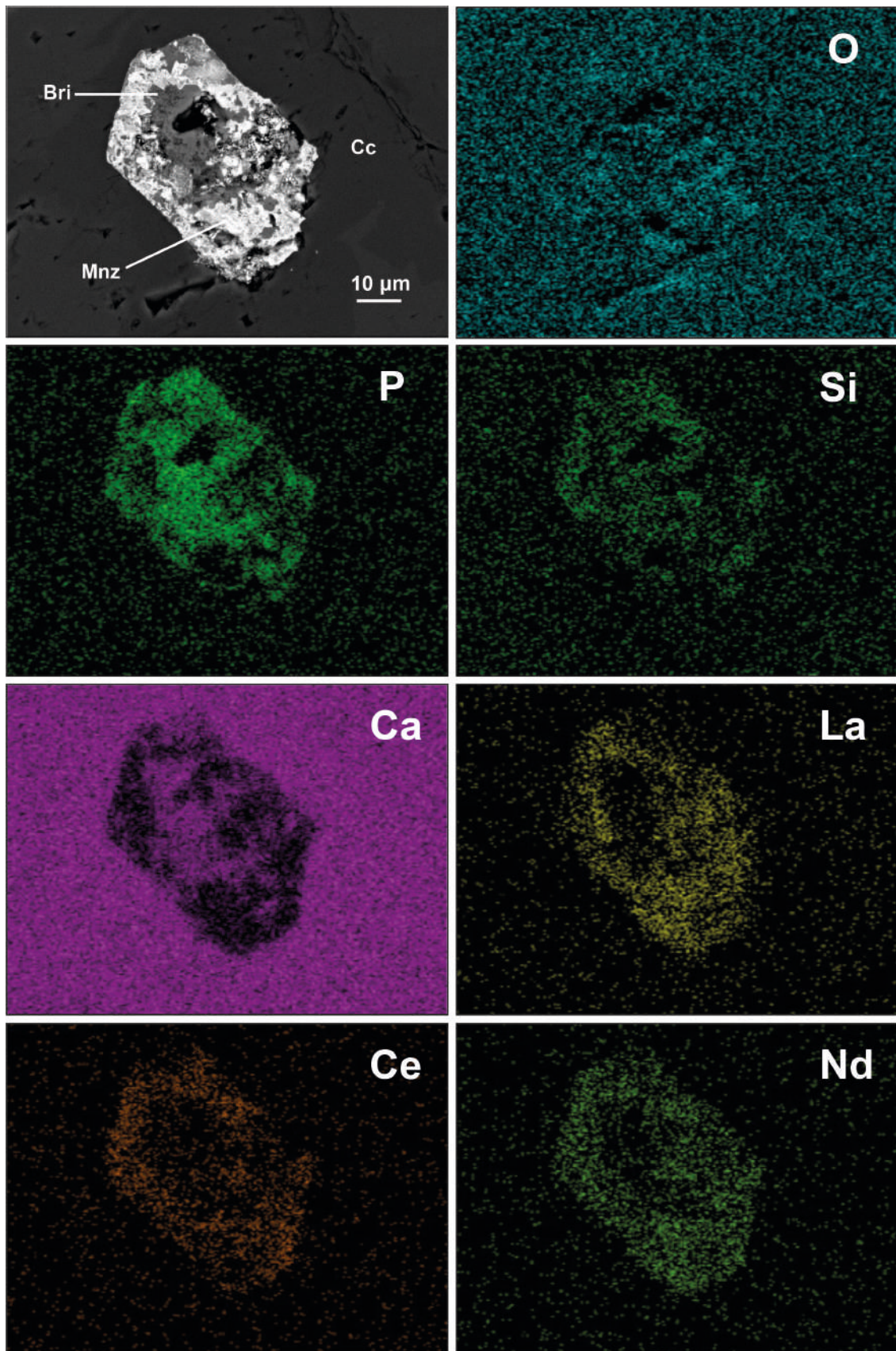
940

941 **Figure 2:** (a), (b) Images showing typical outcrops of the FBC in the southern area of Ajuy (sector 3;
 942 Figure 1). The images highlight characteristic swarms of alkaline and carbonatitic intrusions (whitish)
 943 intersected by later-intruded basaltic dikes (black colour). (c) Detailed view of a carbonatitic dike located
 944 in a shear zone of sector 3, exhibiting distinct linear sigmoidal structures resulting from deformation. (d)
 945 Detailed view of centimetre-sized phlogopite crystals within a carbonatitic dike outcropping in sector 3,
 946 displaying a typical pegmatitic texture. (e) Overview of an outcrop of metric-scale carbonatitic dikes in the
 947 sector 1 area.



949

950 **Figure 3:** SEM (backscattered electron, BSE) images of the Fuerteventura carbonatites. **(a)** Subhedral
 951 crystals of niobium-rich perovskite (Prv-Nb) associated with phlogopite (Phl) and magnetite (Mgt)
 952 aggregates. The association has been affected by secondary hydrothermal processes, leading to the
 953 formation of celestine (Clt). **(b)** Typical subhedral crystal of jacobsite (Jcb) associated with britholite (Bri).
 954 Both crystals are hosted in magmatic calcite (Cc), with numerous disseminated microcrystals of pyrochlore
 955 (Pcl). **(c)** Partially altered subhedral grain of britholite (Bri) hosted in magmatic calcite (Cc). The alteration
 956 process led to the formation of secondary REE phosphates such as monazite-Nd (Mnz-Nd). **(d)** Euhedral
 957 crystal of pyrochlore (Pcl) hosted in calcite (Cc). Brighter areas developed on the grain's borders correspond
 958 to plumbopyrochlore (Pcl-Pb) zonation. **(e)** Typical mineral association related to small skarn like areas
 959 associated with carbonatites. Subhedral zoned crystals of andradite (Adr), hosted in calcite (Cc) and
 960 phlogopite (Phl), with a significant Zr zoning leading to kerimasite (Kms) cores. **(f)** Typical low-
 961 metamorphic alteration developed on carbonatites composed of allanite (Aln) aggregates hosted in calcite
 962 (Cc) and associated with secondary baryte (Brt). Abbreviations of mineral names in all the pictures follow
 963 the criteria proposed by Warr (2021).



965

966

967

Figure 4: Wavelength-dispersive X-ray maps of representative compositional elements for an altered grain of britholite (Bri) hosted in calcite (Cc) and partially transformed into secondary monazite (Mnz).



969

970 **Figure 5:** (a) General view of a typical surface outcrop of Quaternary calcrete located in the Aulagar ravine
971 area (profile B, sector 3; Fig.1). (b) Centimetre-thick calcrete layer filling a fracture between two
972 carbonatitic dikes in the Aulagar ravine area (profile B, sector 3; Fig.1). (c) Calcrete layer developed within
973 fractures between carbonatitic rocks in the Agua Salada ravine area (profile A, sector 1; Fig.1).

974

975

976

977

978

979

980

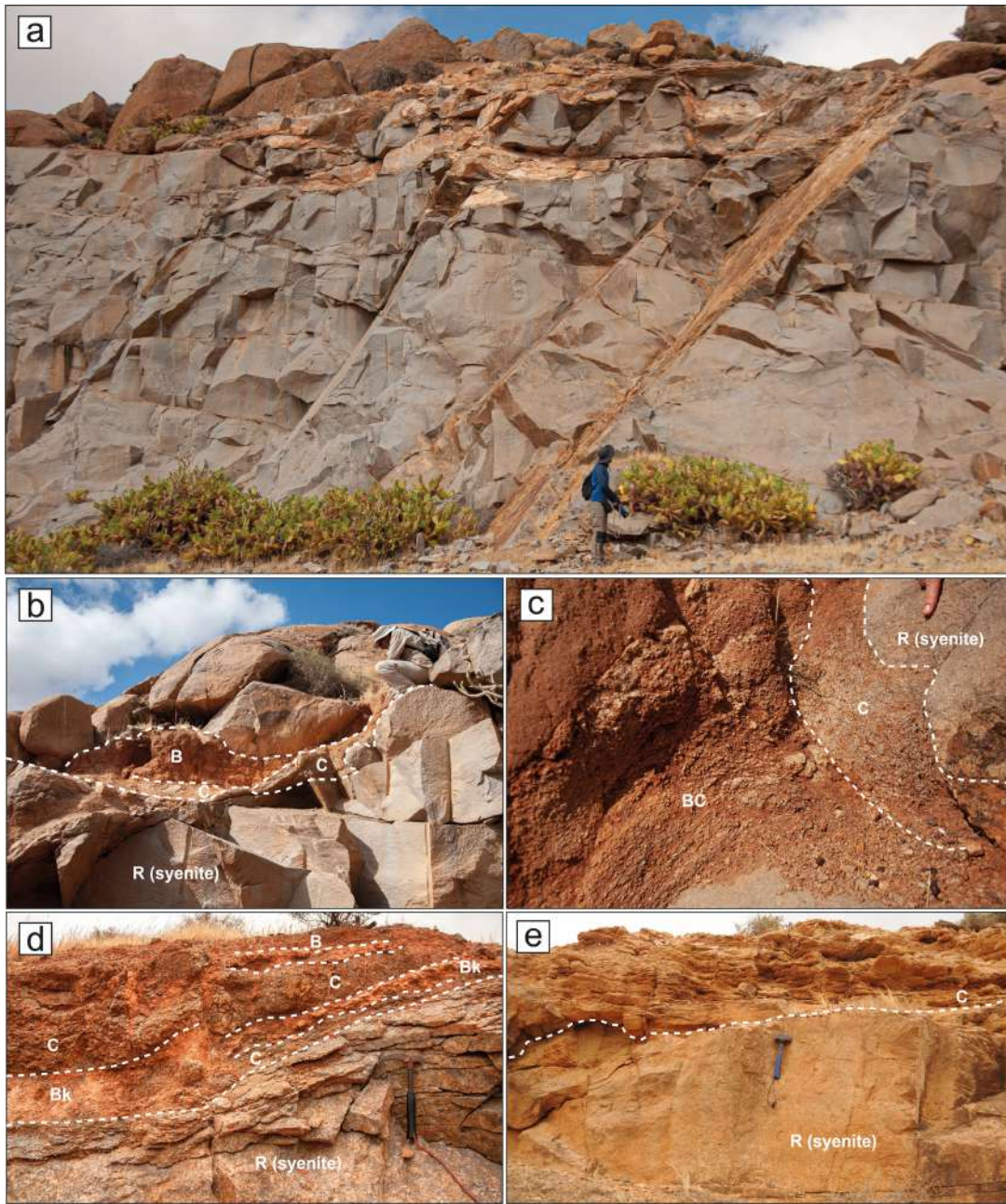
981

982

983

984

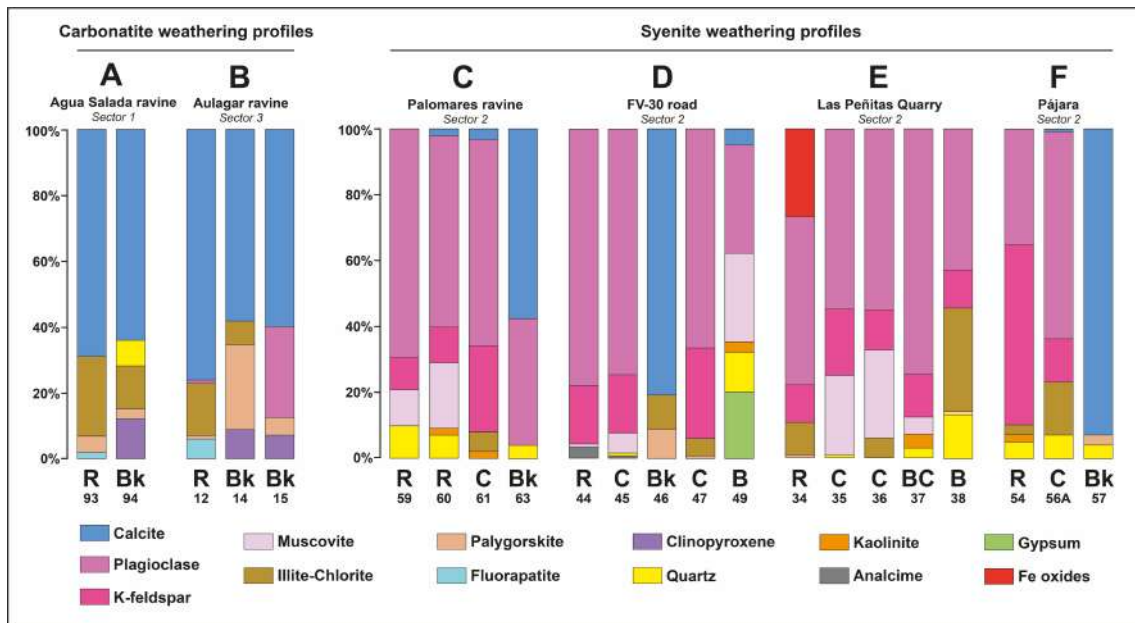
985



987

988 **Figure 6:** (a) General view of Las Peñitas quarry syenite outcrop (profile E, sector 2; Fig.1) where it is
 989 possible to distinguish different fractures filled by injected secondary weathering products. (b) Syenite
 990 weathering profile in Las Peñitas quarry (profile E, sector 2; Figure 1) showing surface erosion and B, BC
 991 and C horizons injected in the syenite bedrock (R). (c) Weathering profile displaying the development of
 992 C and BC horizons associated with a syenite protolith (R), located in Las Peñitas quarry (profile E, sector
 993 2; Figure 1). (d) Weathering profile developed on syenite in the FV-30 road area (profile D, sector 2),
 994 exhibiting the development of C, B and calcrete (Bk) horizons. (e) Weathering profile on syenite protolith
 995 (R) displaying a metric sized C horizon in the Pájara area (profile F, sector 2; Figure 1).

996 **Figure 7**



997

998 **Figure 7:** Graphical mineralogical quantification of the studied weathering profiles: (A) Agua Salada
 999 ravine; (B) Aulagar ravine; (C) Palomares ravine; (D) FV-30 road; (E) Las Peñitas quarry; (F) Pájara. The
 1000 corresponding class assigned to the edaphic horizons (B, BC, Bk, C, R) and the sample number are shown
 1001 at the foot of the columns.

1002

1003

1004

1005

1006

1007

1008

1009

1010

1011

1012

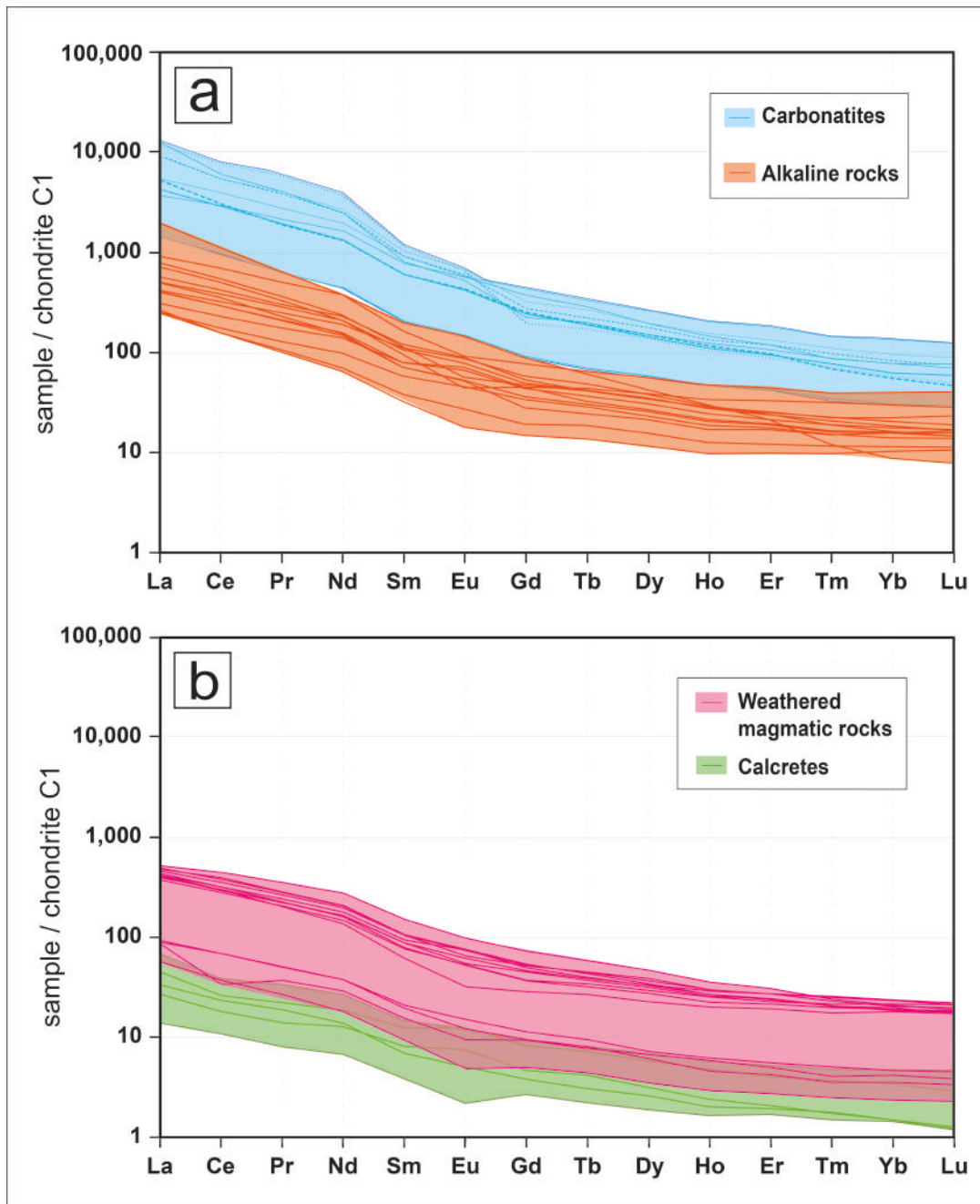
1013

1014

1015

1016

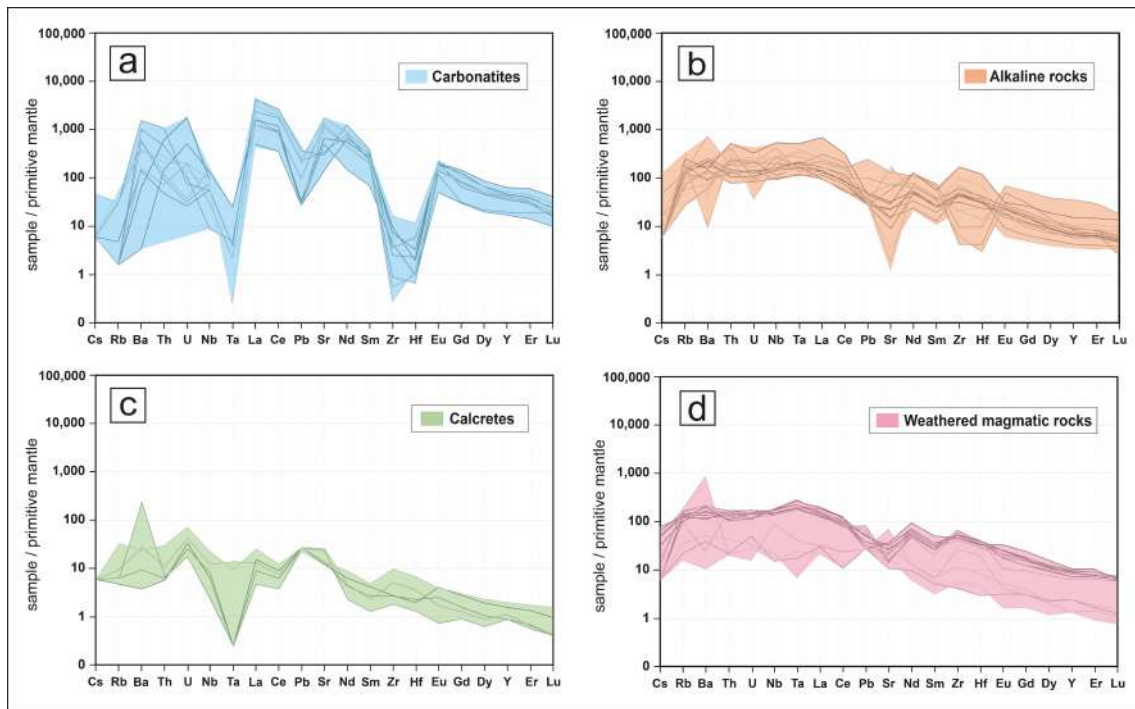
1017



1019
 1020
 1021
 1022
 1023
 1024
 1025
 1026
 1027

Figure 8: REE plots of the studied Fuerteventura lithologies normalised to C1 chondrites. Normalisation values are from McDonough and Sun (1995).

1028 **Figure 9**



1029

1030 **Figure 9:** Multi-elemental trace element plots of Fuerteventura intrusive lithologies normalised to the
1031 primitive mantle. Normalisation values from McDonough and Sun (1995).

1032

1033

1034

1035

1036

1037

1038

1039

1040

1041

1042

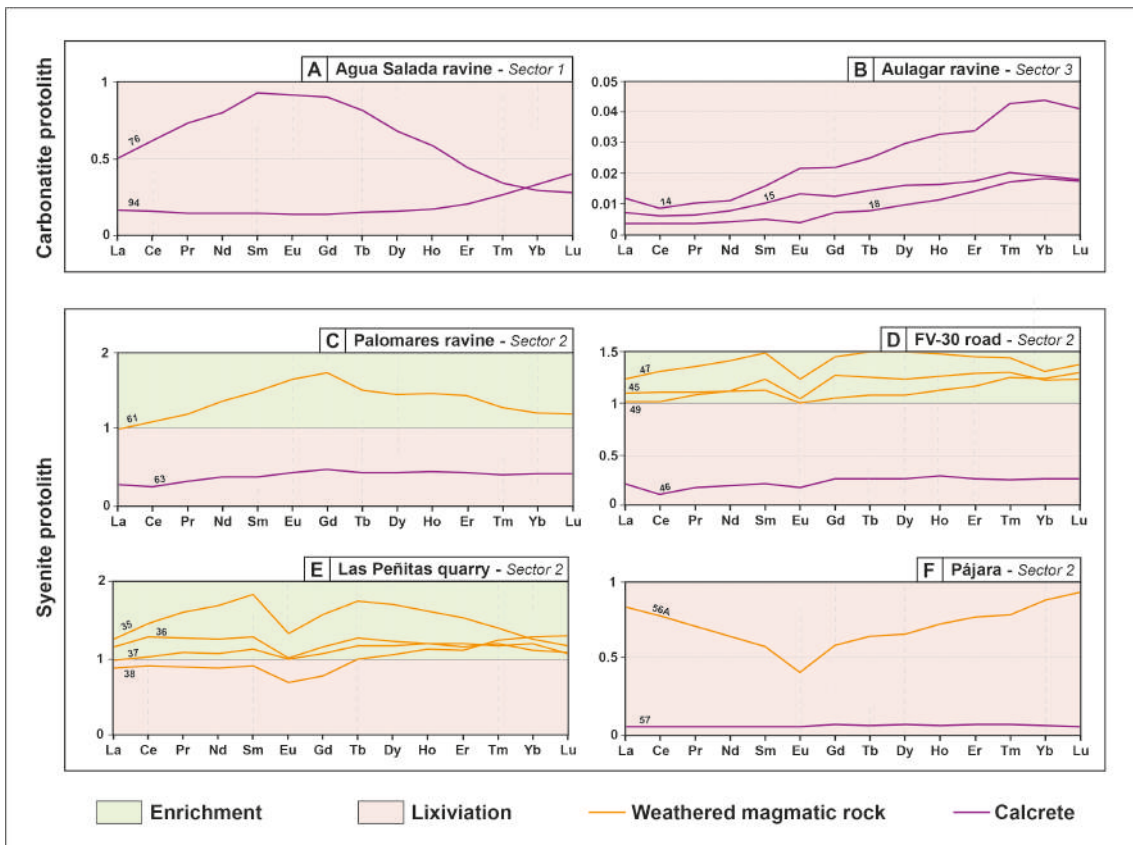
1043

1044

1045

1046

1047



1049

1050 **Figure 10:** REE weathering enrichment/leaching diagrams between primary magmatic protoliths
 1051 (carbonatites and syenites) and the associated weathering products from the studied profiles (Figure 1). The
 1052 sample number is labelled on the corresponding pattern line.

1053

1054

1055

1056

1057

1058

1059

1060

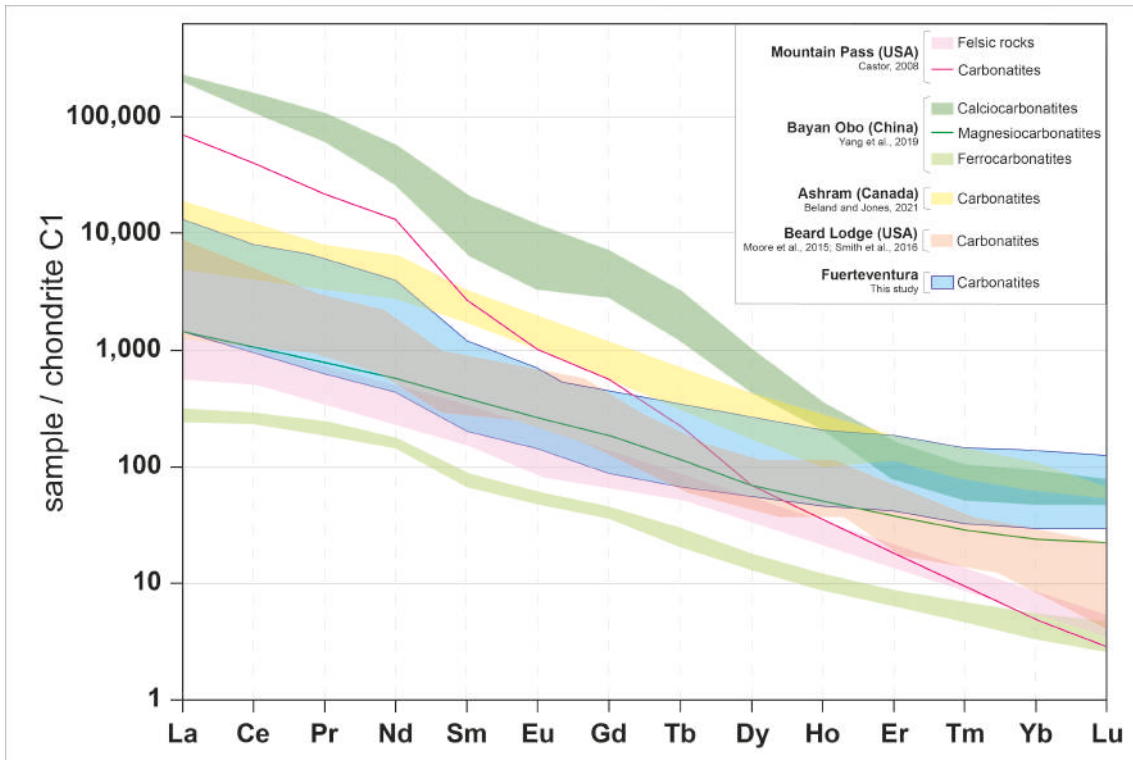
1061

1062

1063

1064

1065 **Figure 11**



1066

1067 **Figure 11:** REE plot of the studied Fuerteventura carbonatites compared to other carbonatitic localities
 1068 worldwide where REE deposits have been reported. REE contents for comparison are from Castor (2008),
 1069 Yang et al. (2019), and Beland and Jones (2021). Normalisation values are from McDonough and Sun
 1070 (1995).